

Article

Regulatory Effects of *GPR158* Overexpression in Trabecular Meshwork Cells of the Eye's Aqueous Outflow Pathways

Maria Fernanda Suarez ¹, Tatsuo Itakura ², Satyabrata Pany ¹, Shinwu Jeong ³, Shraavan K. Chintala ², Michael B. Raizman ⁴, Steven Riesinger ⁵, Tsvetelina Lazarova ⁵, José Echenique ⁶ , Horacio M. Serra ⁶ , W. Daniel Stamer ⁷ and M. Elizabeth Fini ^{8,*}

- ¹ Department of Ophthalmology, Tufts University School of Medicine at Tufts Medical Center, Boston, MA 02111, USA; mf.suarez10@gmail.com (M.F.S.); panysbuh@gmail.com (S.P.)
- ² USC Institute for Genetic Medicine, Keck School of Medicine of USC, University of Southern California, Los Angeles, CA 90007, USA; titakura77@gmail.com (T.I.); shraavan.chintala@gmail.com (S.K.C.)
- ³ Department of Ophthalmology, USC Roski Eye Institute, Keck School of Medicine of USC, University of Southern California, Los Angeles, CA 90007, USA; shinwuje@med.usc.edu
- ⁴ Department of Ophthalmology, Tufts University School of Medicine at Tufts Medical Center and Ophthalmic Consultants of Boston, Boston, MA 02111, USA; michael.raizman@tuftsmedicine.org
- ⁵ MedChem Partners, Lexington, MA 02421, USA; sriesinger@medchempartners.com (S.R.); tlazarova@medchempartners.com (T.L.)
- ⁶ Centro de Investigaciones en Bioquímica Clínica e Inmunología (CIBICI), Department of Clinical Biochemistry, Faculty of Chemistry, National University of Córdoba, Córdoba 5000, Argentina; jechenique@unc.edu.ar (J.E.); horacio.serra@unc.edu.ar (H.M.S.)
- ⁷ Department of Ophthalmology, Duke University, Durham, NC 27708, USA; william.stamer@duke.edu
- ⁸ Department of Ophthalmology, Tufts University School of Medicine at Tufts Medical Center and Programs in Pharmacology & Drug Development and Genetics, Molecular & Cellular Biology, Graduate School of Biomedical Sciences, Tufts University, Boston, MA 02111, USA
- * Correspondence: elizabeth.fini@tuftsmedicine.org



Citation: Suarez, M.F.; Itakura, T.; Pany, S.; Jeong, S.; Chintala, S.K.; Raizman, M.B.; Riesinger, S.; Lazarova, T.; Echenique, J.; Serra, H.M.; et al. Regulatory Effects of *GPR158* Overexpression in Trabecular Meshwork Cells of the Eye's Aqueous Outflow Pathways. *Stresses* **2023**, *3*, 629–652. <https://doi.org/10.3390/stresses3030044>

Academic Editors: Soisungwan Satarug, Aleksandra Buha Djordjevic and Elisa Bona

Received: 27 July 2023

Revised: 29 August 2023

Accepted: 30 August 2023

Published: 1 September 2023



Copyright: © 2023 by the authors. Licensee MDPI, Basel, Switzerland. This article is an open access article distributed under the terms and conditions of the Creative Commons Attribution (CC BY) license (<https://creativecommons.org/licenses/by/4.0/>).

Abstract: Elevated intraocular pressure (IOP), the major risk factor for glaucoma, is caused by decreased outflow through the trabecular meshwork (TM). The pathophysiology of ocular hypertension has been linked to stress pathways, including fibrosis, calcification and the unfolded protein response (UPR). In a pharmacogenomic screen, we previously identified the novel G-protein-coupled receptor (GPCR), *GPR158*, showed that expression is upregulated in TM cells by glucocorticoid stress hormones, and showed that overexpression protects against oxidative stress. We also found that loss of *Gpr158* in knockout mice negates IOP reduction due to treatment with the catecholamine stress hormone, epinephrine. An increase in *GPR158* would be expected to alter the activity of *GPR158*-regulated pathways. Here, we profiled gene expression changes due to *GPR158* overexpression by microarray, then conducted pathway analysis. We identified five upstream stress regulators relevant to ocular hypertension: dexamethasone and TGFβ1 (fibrosis), XBP1 and ATF4 (UPR), and TP53 (cell cycle arrest). Key genes in the first three pathways were downregulated by *GPR158* overexpression, but not enough to inhibit dexamethasone-induced fibrosis or calcification in TM cells, and loss of *Gpr158* in knockout mice only minimally protected against dexamethasone-induced ocular hypertension. Depending on dose, *GPR158* overexpression down- or upregulated the TP53 pathway, suggesting the mechanism for previously observed effects on cell proliferation. A sixth upstream regulator we identified was a GPCR: the beta-adrenergic receptor ADRB1. Adrenergic receptors serve as targets for IOP-lowering drugs, including epinephrine. These data provide new information about pathways regulated by *GPR158*.

Keywords: ocular hypertension; glaucoma; G-protein-coupled receptor; *GPR158*; dexamethasone; TGFβ1; unfolded protein response; TP53; adrenergic receptor; ADRB1

1. Introduction

Elevated intraocular pressure (IOP), also known as “ocular hypertension”, is the major risk factor for glaucoma, the leading cause of irreversible blindness [1], and lowering IOP is the only proven treatment. Ocular hypertension is due to impaired aqueous humor outflow through the trabecular meshwork and Schlemm’s canal [2–7]. While effective pharmaceutical therapeutics exist, some patients do not reach the desired target pressure, even when maximally medicated, indicating a continuing unmet medical need [8].

In open-angle forms of ocular hypertension, such as those that lead to primary open-angle glaucoma (POAG), or steroid-induced glaucoma (SIG) caused by treatment with glucocorticoid stress hormone analogues, pathology is intrinsic to the tissue [9–12]. Pathological changes include loss of cells, collapse of trabecular beams, deposition of extracellular elastin-rich “plaques” (POAG) or fibronectin-rich subcellular deposits (SIG), cytoskeletal rearrangements and the appearance of ACTA2-positive “myofibroblasts” [2–4,6,13–21]. Such changes have been linked to elevated levels of TGFB2 and TGF-beta signaling and lead to tissue stiffening [22–27]. Glucocorticoid upregulation of genes involved in bone ossification has been associated with pathological calcification of trabecular meshwork, and this would also contribute to tissue stiffness [28]. In addition, accumulating evidence implicates endoplasmic reticulum (ER) stress and the unfolded protein response (UPR) as a common pathogenetic mechanism for ocular hypertension leading to POAG [29–32] or SIG [33,34].

Genome-wide association studies (GWASs) have identified over 114 genomic variants associated with POAG and its endophenotypes, including ocular hypertension [35–37]. In a variation on the usual GWAS, we conducted a pharmacogenomic screen for genomic variants associated with steroid-induced ocular hypertension (SIOH). A single-nucleotide polymorphism (rs16925580) located in the first intron of the gene encoding the then novel G-protein-coupled receptor (GPCR), *GPR158*, was identified as a preliminary “hit” [38]. In follow-up studies, we found that *GPR158* is expressed by the immortalized human trabecular meshwork cell line, TM-1, in vitro [39], as well as by trabecular meshwork cells of humans and mice in vivo [40]. Treatment with the glucocorticoid, dexamethasone, stimulated *GPR158* expression in TM-1 cells and primary trabecular meshwork cells in culture. In turn, when ectopically overexpressed in these cells, *GPR158* itself stimulated cell proliferation and knockdown of endogenously expressed *GPR158* inhibited cell proliferation [39]. Similar effects were demonstrated in prostate cancer cell lines [41]. Significantly, *GPR158* overexpression increased survival of TM-1 cells subjected to oxidative stress, a type of stress that has been linked to the pathophysiology of POAG [39]. However, loss of *Gpr158* in knockout (KO) mice (on the C57Bl/6 background) conferred protection against the ocular hypertension that we found to develop as these mice age [40]. These studies suggested that *GPR158* can have both protective and pathological effects on the trabecular meshwork, impacting development of ocular hypertension.

GPCRs discovered via classic biochemical approaches typically couple with heterotrimeric G proteins upon binding of an extracellular activating ligand, thus initiating intracellular signaling. In contrast, so-called “orphan” GPCRs identified via human genome sequencing often exhibit other activities [42,43]. This is the case for *GPR158*, which was shown to act as a scaffold protein for the plasma membrane recruitment of GTPase-activating protein RGS7 via binding of the unconventional G protein GNB5. There RGS7 interacts with GPCRs that bind conventional G proteins of the G α (i/o) class, accelerating their deactivation, thus enhancing cAMP production [44]. Consistent with this mechanism, we showed that *GPR158* overexpression in cultured trabecular meshwork cell enhanced cAMP production in response to the acute stress hormone epinephrine, a conventional GPCR ligand. Furthermore, the IOP-lowering effect of epinephrine, which signals via adrenergic receptors, was negated in *Gpr158* KO mice [40].

An increase in *GPR158* expression, as stimulated by glucocorticoids, would be expected to affect the activity of pathways regulated by this GPCR. The goal of this study was to identify affected pathways that might either be protective or contribute to pathology. We

first profiled gene expression changes due to *GPR158* overexpression in the immortalized TM-1 cell line by microarray screening. Then, we conducted pathway analysis to identify predicted upstream regulators of affected gene sets and we analyzed selected genes in each set more closely. Finally, we conducted functional studies to determine the possible significance of the selected pathways to development of ocular hypertension.

2. Results

2.1. Profiling of *GPR158*-Regulated Gene Expression

To investigate pathways regulated by *GPR158* overexpression in trabecular meshwork cells, we performed microarray-based gene expression profiling using a lentivirus-transformed cell culture model. To create the model, TM-1 cells were infected with a lentiviral construct in which *GPR158* was placed under control of a doxycycline-inducible promoter element; stably transduced clones were selected for use in experiments. Using this approach, the dose of *GPR158* protein received by the cell can be controlled by the concentration of doxycycline used to treat the cells, as well as the duration of treatment.

A schematic outlining the experimental design is shown in Figure 1A. *GPR158* overexpression was induced with doxycycline at 100 ng/mL or 500 ng/mL for 24, 72 or 96 h. A TM-1 cell line stably transduced with empty lentiviral vector, and treated similarly with doxycycline, was also profiled to ensure observed changes in gene expression were not due to doxycycline alone.

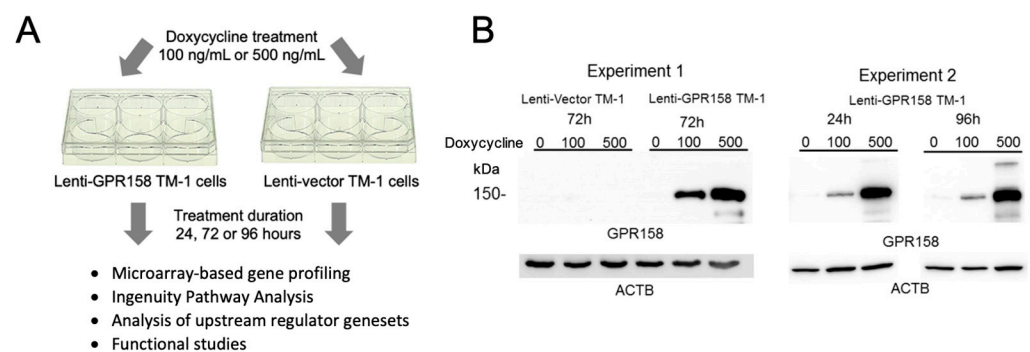


Figure 1. Profiling of *GPR158*-induced gene expression in TM-1 cells. (A) Experimental and analytical design for the *GPR158*-regulated pathway analysis utilizing the paired lenti-*GPR158* TM-1 and lenti-vector TM-1 cell lines. (B) Immunoblot documenting *GPR158* protein levels induced in the two experiments.

Elevation of the *GPR158* protein level was documented in each experiment by immunoblotting, as shown in Figure 1B. From this analysis, it can be seen that the 100 ng/mL and 500 ng/mL doxycycline concentrations induced *GPR158* protein accumulation to approximately the same level; however, cells were exposed to this level of protein for different lengths of time in the different experiments.

Following expression profiling, the genes that were differentially expressed in response to *GPR158* overexpression were identified by comparing microarray gene expression values for vehicle-treated lenti-*GPR158* to doxycycline-treated lenti-*GPR158*.

Next, we imported the microarray data into the Ingenuity Pathway Analysis (IPA) software. Top upregulated and downregulated genes, with fold change in expression, are shown in Table S1. We next used IPA's upstream regulator tool, which identifies gene sets from the total differentially expressed genes that are known to be controlled by specific proteins or small molecules ("upstream regulators"). We selected five stress-regulated pathways for follow-up based on their relevance to ocular hypertension and previous trabecular meshwork cell culture findings; these are listed in Table 1.

Table 1. Selected upstream stress regulators identified by IPA.

GPR158 Dose	Exp 1	Exp 2A	Exp 2B
Doxycycline	Low	High	High
Duration	72 h	24 h	96 h
IPA Top Upstream Regulators			
Dexamethasone	$p = 2.71 \times 10^{-9}$	$p = 4.55 \times 10^{-17}$	$p = 1.62 \times 10^{-6}$ activated
TGFB1	$p = 1.19 \times 10^{-9}$	$p = 1.02 \times 10^{-23}$	$p = 2.54 \times 10^{-16}$ inhibited
XBP1			$p = 1.09 \times 10^{-5}$ inhibited
ATF4			$p = 5.46 \times 10^{-6}$
TP53	$p = 1.13 \times 10^{-5}$	$p = 4.84 \times 10^{-18}$ inhibited	$p = 3.41 \times 10^{-15}$ activated

The *p*-value indicates the overlap of GPR158-regulated gene sets with those regulated by the IPA-identified “upstream regulator”. If the pathway is predicted by IPA to be activated or inhibited, this is indicated.

Next, we sought to validate selected differentially expressed genes and IPA pathways identified. Representative results are shown in Figure 2. First, lenti-GPR158 TM-1 cells were treated to achieve the three GPR158 doses used for microarray analysis, then the change in gene expression was quantified by qPCR for select genes and fold change compared to the microarray result (Figure 2A). In addition, the paired TM-1 cell lines (lenti-vector and lenti-GPR158) were treated with doxycycline at 500 ng/mL over a time course of 24–96 h, then the accumulation of protein products of select genes was evaluated by immunoblotting (Figure 2B).

COL10A1 was one of the genes identified by microarray as most highly upregulated at the moderate GPR158 dose (Table S1); it was also upregulated at the highest dose, but its expression was not significantly affected at the lowest dose. This finding was validated by qPCR (Figure 2A) and immunoblotting (Figure 2B). *CA12* was one of the top downregulated genes at the lowest dose of GPR158 (Supplementary Materials Table S1), and was also downregulated at moderate and high doses. This finding was validated by qPCR (Figure 2A). *SLC8A2* was one of the genes identified by microarray as most highly upregulated at the moderate GPR158 dose. This finding was validated by immunoblotting (Figure 2B).

Expression of the gene encoding upstream regulator TGFB1 was not observed to be changed by microarray analysis. However, expression of *TGFB2*, encoding a cytokine with similar activity whose expression changes in the trabecular meshwork from eyes with ocular hypertension and glaucoma [22–27], was downregulated at the moderate GPR158 dose (Figure 2A). This validated the microarray result. It was also consistent with the IPA prediction of TGFB1 pathway inhibition (Table 1), since one would expect downregulation of the upstream regulator.

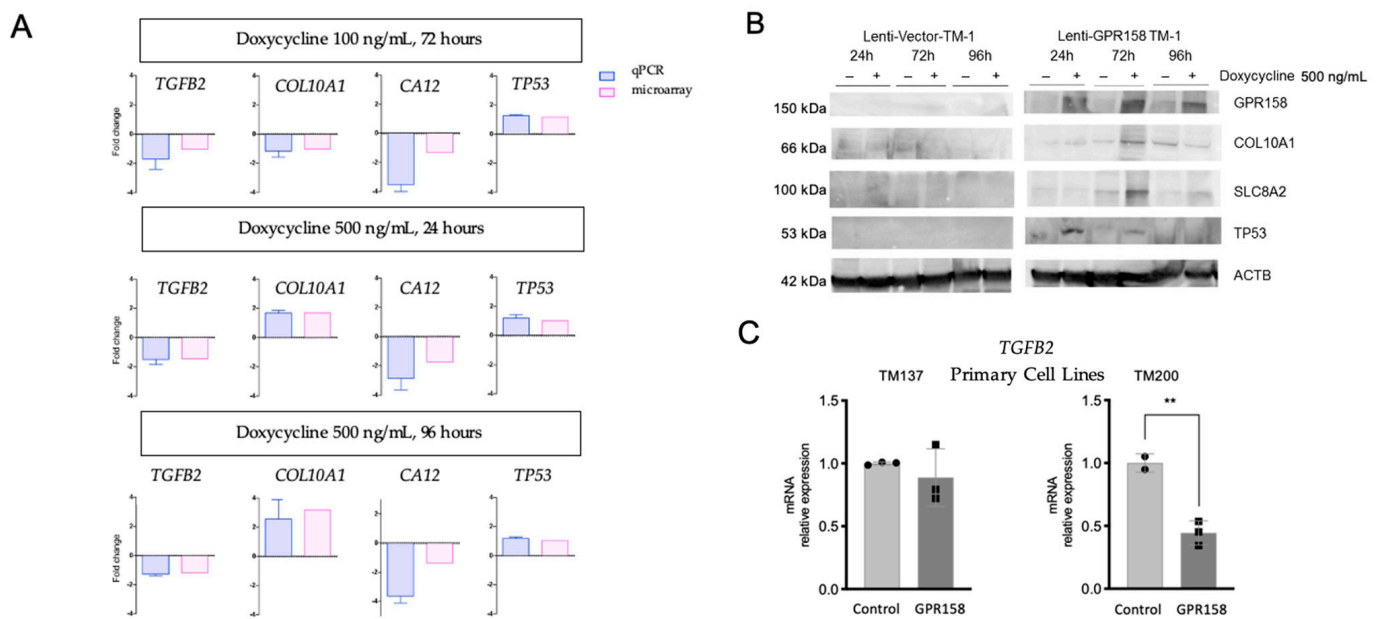


Figure 2. Validation of microarray and IPA upstream regulator results. (A) qPCR validation of microarray and IPA data for selected genes using the lenti-GPR158 TM-1 cell line. N = 3. (B) Immunoblot validation of microarray and IPA data for selected genes using the lenti-GPR158 TM-1 cell line. (C) qPCR validation of microarray and IPA data for *TGFB2* using two primary cell strains, TM137 and TM200. Cells were transiently transfected with a GPR158 expression vector or empty vector control. After 48 h, RNA was extracted for qPCR. Student *t*-test; $n = 3$; ** $p < 0.01$. For TM200, $p = 0.0064$.

We also sought to validate the observed GPR158-induced decrease in *TGFB2* expression in primary trabecular meshwork cells in culture. For this, *GPR158* was overexpressed by transient transfection in two different primary cells strains: TM137 and TM200 (Figure 2C). *TGFB2* mRNA was decreased by transient *GPR158* overexpression in both cell strains; the decrease was statistically significant in TM200 cells. Differences between primary cell lines likely reflect genetic differences among individuals.

Expression of the gene encoding the upstream regulator, TP53, was unchanged by GPR158 overexpression as determined by qPCR (Figure 2A); however, the protein level was clearly increased as determined by immunoblotting (Figure 2B). This is consistent with the known mechanism of TP53 pathway activation; TP53 protein is stabilized in response to cellular stress [45].

2.2. IPA Upstream Stress Regulator Analysis

In our next analyses, we looked more closely at the gene sets associated with the five selected upstream stress regulators. Tables 2–4 list differentially expressed genes that IPA includes as part of the selected gene sets, showing fold change in gene expression (+ or –) due to overexpression of *GPR158*, as observed in microarray experiments 1 and 2 (Figure 1).

Table 2. Selected genes from IPA “top upstream regulator” findings: dexamethasone regulated, TGFB1 regulated.

Gene	Fold Change in Gene Expression			Change Direction Predicted	Change Direction Observed
	Exp 1 Low, 72 h	Exp 2A High, 24 h	Exp 2B High, 96 h		
Dexamethasone regulated					
Acute					
<i>AKR1C1/C2</i>	−1.302	−1.991	−1.503	up	down
<i>AKR1C3</i>	−1.443	−1.625		up	down
<i>AKR1C4</i> *	−1.313	−2.206	−1.576	up *	down
<i>CA12</i> **	−1.317	−1.727	−1.362	up	down
<i>CHI3L1</i>	−1.370	−1.571		up	down
Extracellular matrix					
<i>ADAMTS1</i>		−1.229		up	down
<i>COL1A1</i>		−1.250		up	down
<i>COL4A1</i>	−1.276	−1.256		up	down
<i>COL4A5</i>			+1.256	up	up
<i>COL10A1</i>		+1.686	+3.183	down	up
<i>LAMA4</i>	−1.218	−1.218	−1.212	up	down
<i>LAMA5</i>	−1.212	−1.394	+1.220	up	regulates
<i>VCAN</i>	−1.235	−1.570	−1.786	down	down
Growth factors and matricellular proteins					
<i>CTGF</i>	−1.144	−1.320		up	down
<i>CYR61</i>	−1.211	−1.292	+1.315	regulates	regulates
<i>GDF15</i>	+1.354		+1.374	down	up
<i>TGFB2</i>		−1.443		up	down
<i>THBS1</i>	−1.242	−1.363	+1.249	up	regulates
<i>WNT5A</i>	−1.264			up	down
<i>WNT5B</i> ***	−1.212	−1.376		---	down
TGFB1 regulated					
Extracellular matrix					
<i>COL1A1</i>		−1.250		up	down
<i>COL3A1</i>			−1.594	up	down
<i>COL4A1</i>	−1.276	−1.256		up	down
<i>COL5A1</i>			−1.254	up	down
<i>COL6A3</i>			−1.539	up	down
<i>VCAN</i>		−1.570	−1.786	down	down
Growth factors and matricellular proteins					
<i>BMP4</i>	−1.212	−1.382		down	down
<i>DACT3</i> ****		+1.457	+1.228	---	up
<i>DKK3</i>			+1.262	up	up
<i>GDF15</i>	+1.354		+1.374	up	up
<i>THBS1</i>	−1.242	−1.363	+1.249	up	regulates

Shown are differentially expressed genes with the fold change in gene expression (+ or −) in each of the experiments. If a table cell is gray, the change in gene expression was not statistically significant. The direction of change in dexamethasone-induced gene expression predicted by IPA and actual change in direction observed is indicated. * AKR1C4 downregulated by dexamethasone according to IPA, but upregulated in TM-1 cells by dexamethasone and other glucocorticoids according to publications cited in the text; ** not identified as dexamethasone regulated by IPA, but upregulated in TM-1 cells by dexamethasone and other glucocorticoids, as cited in the text; *** not identified as dexamethasone regulated by IPA; **** not identified as TGFB1 regulated by IPA, but is a known negative regulator of TGF-beta signaling.

Table 3. Selected calcification-related genes regulated by *GPR158* overexpression.

Gene	Fold Change in Gene Expression			Change Direction Predicted	Change Direction Observed
	Exp 1 Low, 72 h	Exp 2A High, 24 h	Exp 2B High, 96 h		
Calcification related					
<i>ACTG2</i>	−1.204		−1.414	up	down
<i>ALPL</i>		+1.340		up	up
<i>ALPP</i>			+1.578	up	up
<i>BGLAP</i>				---	---
<i>BMP2</i>				up	---
<i>BMP4</i>	−1.212	−1.382		up	down
<i>COL1A1</i>		−1.250		up	down
<i>COL10A1</i>		+1.686	+3.183	up	up
<i>ECM1</i>			+1.319	up	up
<i>MGP</i>		−1.221		down	down
<i>OSTF1</i>		+1.203		down	up
<i>SLC8A2</i>		+2.174	+1.777	down	up
<i>TNFRSF11B</i>	−1.215			down	down
<i>WNT5A</i>	−1.264			up	down
<i>WNT5B</i>	−1.212	−1.376		up	down

Shown are differentially expressed genes with the fold change in gene expression (+ or −) in each of the experiments. If a table cell is gray, the change in gene expression was not statistically significant. The direction of change in dexamethasone-induced gene expression predicted by IPA and actual change in direction observed is indicated.

Table 4. Selected genes from IPA “upstream regulator” findings: TP53 regulated.

Gene	Fold Change in Gene Expression			Change Direction Predicted	Change Direction Observed
	Exp 1 Low, 72 h	Exp 2A High, 24 h	Exp 2B High, 96 h		
TP53-regulated					
Cell cycle progression					
<i>CCNA1</i> ****			−1.956	---	down
<i>CCNA2</i>			−1.368	down	down
<i>CCNB2</i>			−1.269	regulates	down
<i>CCND1</i>		−1.292		regulates	down
<i>CCNE1</i>			−1.258	regulates	down
<i>CDC25C</i>			−1.371	down	down
<i>MYC</i>		−1.707	−1.268	down	down
Cell cycle arrest					
<i>BRSK1</i>		+1.475	+1.335	up	up
<i>CDC42EP5</i>		+1.708	+1.547	up	up
<i>CDKN1A</i>		−1.186	+1.264	up	up
<i>GAS1</i>	−1.516	−1.513		regulates	down
<i>KLF6</i>		−1.818		up	down
<i>MAPRE3</i>		−1.357	+1.219	up	regulates
<i>SIRT4</i>		+1.433	+1.306	up	up
<i>TP53</i>				up	---
<i>TXNIP</i>		−1.427	+9.300	up	regulates
Mitosis					
<i>CDC20</i>			−1.255	down	down
<i>CENPF</i>			−2.203	down	down
<i>CEP55</i>			−1.236	down	down
<i>AURKA</i>			−1.259	down	down
<i>PEG10</i>		−1.235	−1.410	down	down

Shown are differentially expressed genes with the fold change in gene expression (+ or −) in each of the experiments. If a table cell is gray, the change in gene expression was not statistically significant. The direction of change in dexamethasone-induced gene expression predicted by IPA and actual change in direction observed is indicated. **** Not identified as TP53 regulated by IPA.

2.2.1. Upstream Stress Regulators: Dexamethasone and TGFB1 (Fibrosis)

As noted in the Introduction, *GPR158* was identified in a screen for genes associated with SIOH, and TGFB2 has been implicated as a regulator of the pathological fibrotic response that characterizes open-angle forms of ocular hypertension, including SIOH. TGFB1 is a cytokine with similar activity as TGFB2, both members of the TGF-beta superfamily. For these reasons, we considered the IPA-identified upstream regulators dexamethasone and TGFB1 as highly significant. Table 2 compiles examples of differentially expressed genes from the dexamethasone and TGFB1 upstream regulator gene sets, with the fold change in gene expression (+ or –) observed in each of the experiments. If a table cell is gray, the change in gene expression was not statistically significant.

The “acute” subcategory for dexamethasone in Table 2 compiles differentially expressed genes with immediate effects on IOP. This includes genes encoding four members of the aldo-keto reductase superfamily (AKR1C1–4). The IOP-lowering drug, bimatoprost, is a structural analogue of the AKR1C3 product prostaglandin F2alpha, and inhibits AKR1C3 activity in raising IOP [46]. Other differentially expressed included in this category are *CHI3L1*, encoding a trabecular meshwork cell-secreted protein found at high levels in the aqueous humor [47], and *CA12*, encoding a carbonic anhydrase involved in aqueous humor production, overexpression of which has been associated with elevated IOP in glaucoma [48]. These genes are predicted by IPA to be upregulated by dexamethasone and their upregulation has been documented specifically in trabecular meshwork cell cultures treated with glucocorticoids [49–53]. Significantly, these genes were all downregulated by *GPR158*, at all doses.

A second subcategory in Table 2 compiles differentially expressed genes encoding extracellular matrix. The lists includes genes encoding seven collagen subtypes and two laminins, as well as *VCAN* (versican), an important component of aqueous outflow resistance in the trabecular meshwork [54]. The gene encoding *ADAMTS1* was also on the dexamethasone list. Members of the metzincin superfamily of extracellular matrix-degrading proteinases, *ADAM* and *ADAMTS*, have been implicated in regulation of aqueous outflow [17]. Significantly however, essentially all these differentially expressed genes were downregulated by *GPR158* overexpression. There were two exceptions: genes encoding the collagen subtypes *COL4A5* and *COL10A1* were both upregulated at the higher *GPR158* dose.

A third subcategory in Table 2 compiles differentially expressed genes encoding growth factors and matricellular proteins, i.e., extracellular matrix proteins that play regulatory roles to control extracellular matrix deposition. Several have been specifically implicated in ocular hypertension. This includes genes encoding TGF-beta superfamily member TGFB2 [22,55,56], the matricellular protein THBS1 [57], and growth factor WNT5A and its inhibitor DKK [58]. As a group, these genes are predicted by IPA to be upregulated by dexamethasone and TGFB1. However, they were essentially all downregulated by *GPR158* (*DKK* was correspondingly upregulated). There were two exceptions: The gene encoding TGF-beta superfamily member *GDF15* was upregulated at low and high *GPR158* doses, and the gene encoding matricellular protein THBS1 was upregulated at the highest dose of *GPR158*.

As noted in the Introduction, glucocorticoid regulation of genes involved in bone ossification has been associated with pathological calcification of trabecular meshwork, and this could contribute to tissue stiffness. As we examined dexamethasone and TGFB1-regulated gene sets (Table 2), we noted a number of ossification-associated genes were present, in particular, two of the most highly upregulated genes: *COL10A1* and *SLC8A2* (Table S1). We then went back to the IPA results and observed that the combined IPA for all three experiments identified a “Top Tox Function” as “Increased Levels of Alkaline Phosphatase” with a *p*-value of 4.07×10^{-3} to 4.07×10^{-3} . We then turned to the previously published microarray profile to make comparisons [28]. Table 3 compiles genes that were found to be differentially expressed when trabecular meshwork cells are treated with

glucocorticoids, that are associated with calcification, and that were also differentially expressed by *GPR158* overexpression in the current study.

Only approximately half of the genes listed in Table 3 were regulated in the direction predicted to stimulate calcification. The activity of alkaline phosphatase, a key regulator of soft tissue calcification, is increased in trabecular meshwork cells treated with dexamethasone or TGFB2 in culture [59,60]. In agreement with this, *ALPL* and *ALPP*, both of which encode alkaline phosphatases, were upregulated by *GPR158* overexpression (Table 3) as predicted by the IPA. Stimulated expression of two of the most highly induced genes in this analysis, *COL10A1* and *SLC8A2*, is also documented here at the protein level (Figure 2D). BGLAP is a protein hormone that is highly expressed during the last stages of bone formation and it has been reported to be expressed at low levels by cells of the trabecular meshwork [28]. We observed expression of the *BGLAP* gene here, but this was not altered by *GPR158* overexpression.

2.2.2. Upstream Stress Regulators: XBP1 and ATF4 (UPR)

As noted in the Introduction, accumulating evidence implicates UPR activation as a common pathogenic mechanism for ocular hypertension leading to POAG and in SIOH. The schematic in Figure 3A summarizes the steps in UPR activation. Normally, UPR activation protects the cell. However, if ER stress continues unresolved, programmed cell death is orchestrated by induced expression of *DDIT3*. This is thought to contribute to the pathology of ocular hypertension that ultimately leads to POAG.

UPR pathway components ATF4 and XBP1 were among the IPA top upstream regulators (Table 1). *HSPA5* and *DDIT3* were among the top downregulated genes (Table S1). In our next set of experiments, we evaluated the effects of *GPR158* overexpression at low dose in TM-1 cells and after transient transfection into our primary cell lines. Representative results are shown in Figure 3B–D.

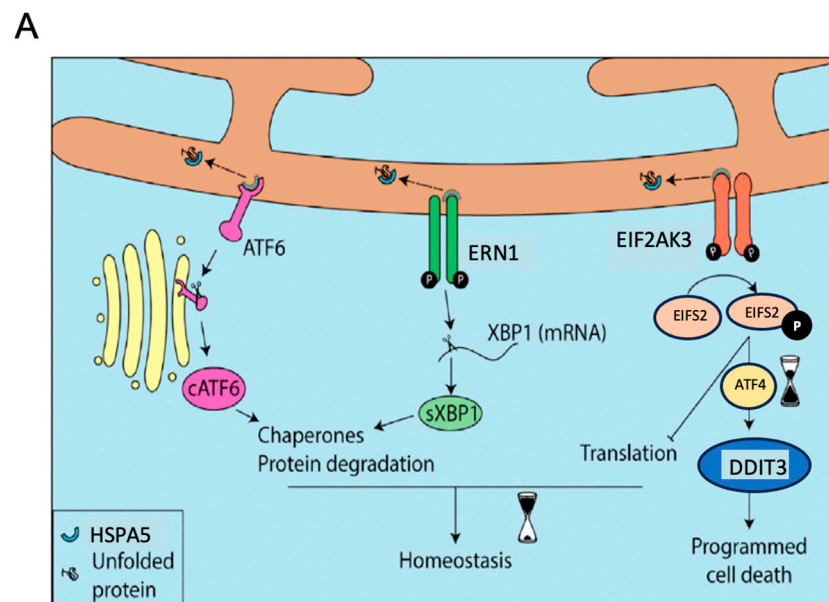


Figure 3. Cont.

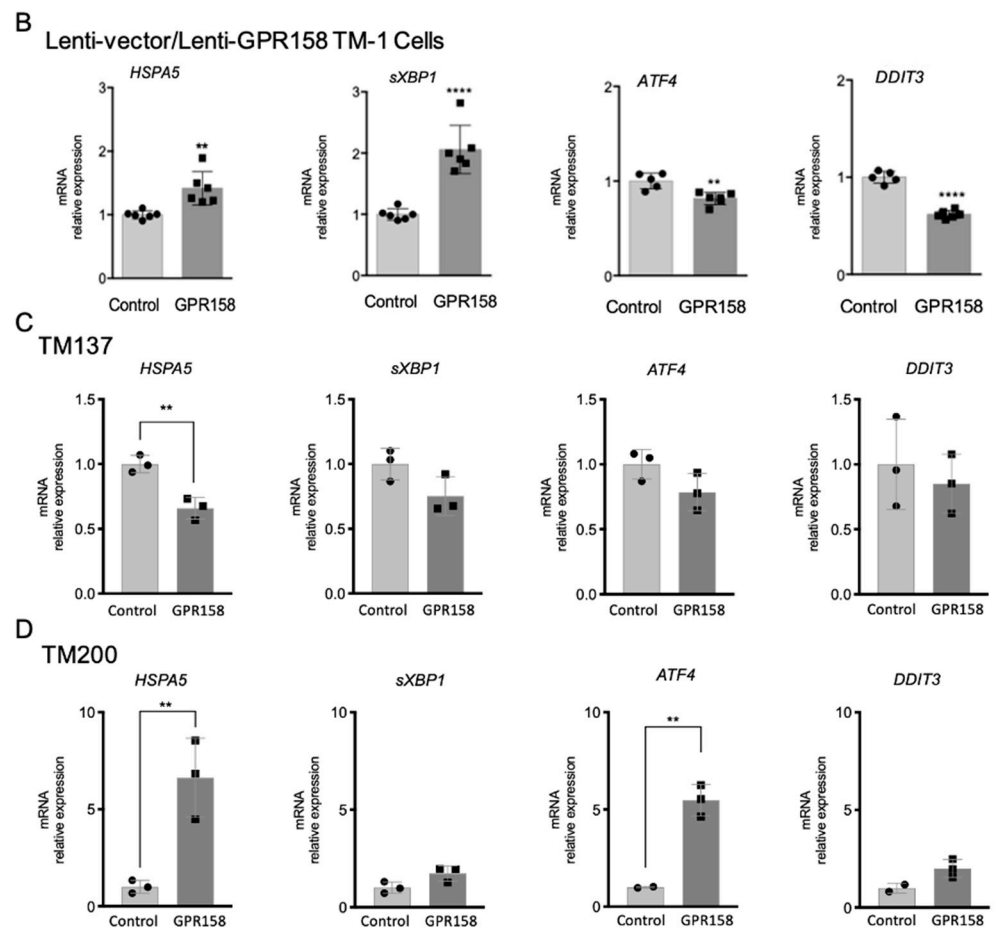


Figure 3. GPR158 overexpression regulates the UPR in trabecular meshwork cells. (A) Schematic of the UPR. HSPA5 (also known as GRP78 or BiP) normally maintains UPR sensor proteins ATF6, ERN1 and EIF2AK3 in an inactive state. However, when misfolded proteins accumulate, the sensors are released and activated, resulting in production of second messengers: proteolytically cleaved ATF6 (cATF6), alternatively spliced XBP1 (sXBP1), and phosphorylated EIFS2 (EIFS2-P). Signaling by these second messengers results in increased production of molecular chaperones, activation of ER-associated protein degradation (ERAD), and a reduction in protein translation, thus helping to restore homeostasis. However, when ER stress is prolonged (as represented by the hour glass icon), phosphorylated EIFS2 leads to induced expression of DDIT3 (also known as CHOP), which causes cell death (reviewed in [61,62]). (B) *GPR158* expression was induced by exposing lenti-GPR158 TM-1 cells (GPR158) or lenti-vector TM-1 cells (Control) to 100 ng/mL doxycycline for 72 h. Alternatively, *GPR158* expression was induced by transient transduction with a *GPR158* expression vector in primary cell strains (C) TM137 or (D) TM200, followed by 24 h of incubation. At the experimental endpoint, RNA was extracted and qPCR was performed to test the mRNA expression level for *HSPA5*, *sXBP1*, *ATF4*, and *DDIT3*. $n = 3-6$. Statistical significance was determined by ANOVA; ** $p < 0.01$; **** $p < 0.0001$.

In TM-1 cells (Figure 3B), we found that *HSPA5* mRNA was upregulated at the lowest dose of GPR158, the opposite of the result obtained at the highest GPR158 dose (Table S1). However, expression of other markers was similar at both doses. Thus, the spliced form of *XBP1* mRNA (*sXBP1*) was upregulated, and both *ATF4* and *DDIT3* mRNAs were down-regulated. When GPR158 was transiently transfected into the TM137 primary trabecular meshwork cell line (Figure 3C), *HSPA5* mRNA was decreased, with no effect on the other markers. In contrast, transient transfection of GPR158 into TM200 cell increased mRNA for both *HSPA5* and *ATF4*, with no effect on the other markers (Figure 3C). As noted previously

(Figure 2), differences between primary cell lines likely reflect known genetic differences among individuals.

These results indicate that *GPR158* overexpression differentially regulates UPR marker expression at low and high doses in TM-1 cells, as well as in primary cell lines. In all cases, however, a protective effect is predicted because *DDIT3* expression is either reduced or unaffected.

2.2.3. Upstream Stress Regulator: TP53

As noted in the Introduction, we previously observed that transient transfection with GPR158 stimulates cell proliferation in trabecular meshwork and prostate cancer cells. However, in the lentivirus stably transformed model, low-dose GPR158 (100 ng/mL doxycycline) stimulates cell proliferation, high-dose GPR158 (500 ng/mL doxycycline) reverses this. The tumor suppressor TP53 arrests cell replication by holding the cell cycle at the G1/S regulation point through its action as a transcription factor when activated by a variety of cell stresses [45]. This suggested TP53 as a candidate mediator of the observed reversal of cell proliferation, and was responsible for our interest in this pathway.

Table 4 lists selected genes regulated by *GPR158* overexpression that overlap with the TP53-regulated gene set. The first subcategory compiles genes encoding positive cell cycle regulators including five cyclins, as well as *CDC25C*, encoding a protein that directs dephosphorylation of cyclin B-bound CDC2 and triggers entry into mitosis. Expression of these genes was not activated, but this is not inconsistent with cell proliferation as cyclin activity is regulated at the protein level [63], similarly to TP53 [45]. This category also includes the gene encoding the cell cycle-regulating transcription factor MYC. TP53-mediated downregulation of MYC expression is essential for cell cycle arrest [64]. At the highest dose of GPR158, all but one gene was significantly downregulated. A second subcategory encodes genes that cause cell cycle arrest. These genes were similarly upregulated at higher GPR158 doses. The last subcategory compiles examples of genes whose protein products are involved with the mechanics of chromosomal replication and mitosis. These genes were similarly regulated as the other categories.

These findings are consistent with the idea that activation of the TP53 pathway is responsible for inhibition of cell proliferation at high doses of GPR158 [41].

2.3. Functional Studies

Our previous observation that *GPR158* expression is induced by dexamethasone (as noted in the Introduction), and our observation here, that fibrosis-associated genes regulated by dexamethasone are downregulated by *GPR158* overexpression, suggested that *GPR158* overexpression might reverse the fibrosis-inducing effects of dexamethasone. We investigated this hypothesis using our lentivirus-transduced TM-1 cell model. Representative results are shown in Figure 4A. The fibrotic response due to dexamethasone treatment of TM cells is specifically characterized by deposition of the fibronectin protein FN1. Dexamethasone treatment induced expression of *FN1* to a significant level, however *GPR158* overexpression did not significantly reverse this.

We also followed up on our finding here that *GPR158* overexpression regulates genes associated with calcification. To detect any calcification, we performed alizarin red staining on lenti-GPR158 TM-1 cell cultures after delivering the same three GPR158 doses used in our microarray experiments. However, no calcium staining was observed (data not shown).

To investigate effects of GPR158 deficiency on SIOH, we utilized *Gpr158* KO mice. We treated these mice with glucocorticoids in two ways: first, by application of dexamethasone eyedrops and, second, by injection of dexamethasone loaded nanoparticles. Then, we also tried both eye drops and nanoparticles together. Results are shown in Figure 4B. In both KO mice and wild-type littermates, IOP increased with dexamethasone treatment. Over the entire time course, the IOP for *Gpr158* KO mice was typically slightly higher than for wild-type littermate mice. However, it was only at the 3 day time point in the experiment that utilized treatment with Dex-NPs that this difference was statistically significant. Thus,

only minimal protection against dexamethasone-induced ocular hypertension was afforded by loss of *Gpr158* in KO mice

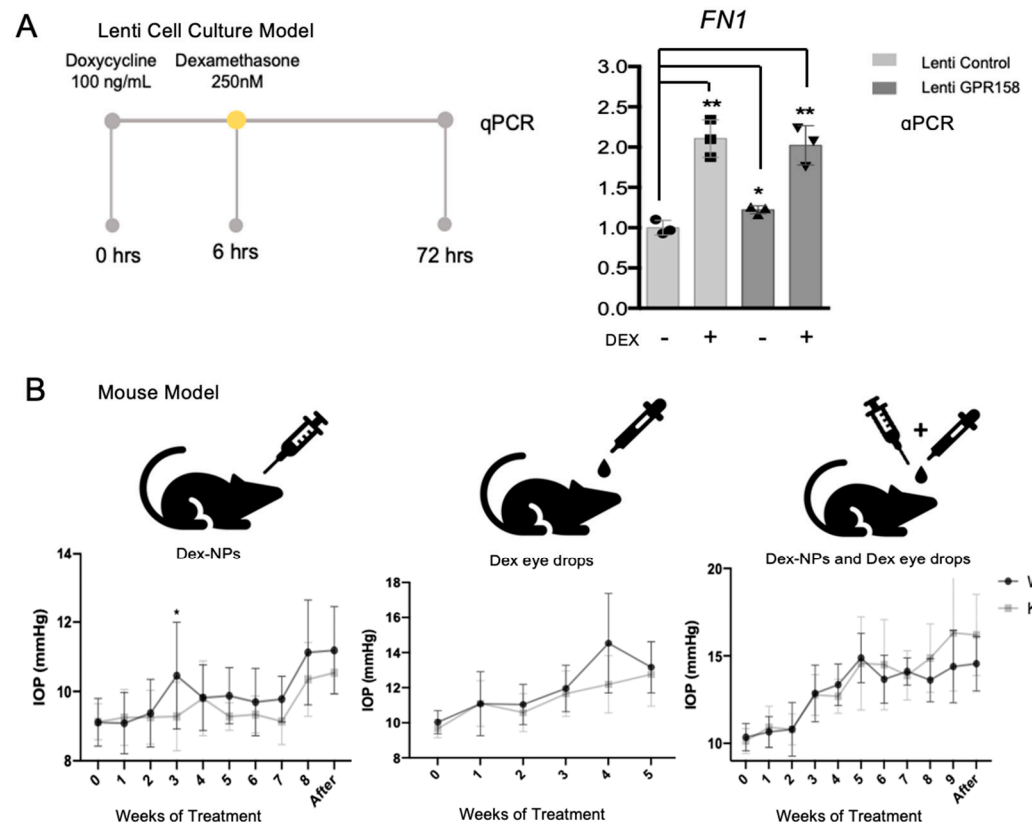


Figure 4. Assessment of the effects of GPR158 on the dexamethasone-induced fibrotic response and on development of SIOH. **(A)** Cell culture model. **(Left Panel)** GPR158 expression was induced by exposing the lenti-GPR158 TM-1 cell line to 100 ng/mL doxycycline for 6 h. The lenti-vector TM-1 cell line was also exposed to doxycycline for comparison. After this, cells were left untreated or treated with dexamethasone (250 nM) for 72 h. Then, mRNA was extracted and qPCR was performed to compare accumulated mRNA for specific genes. **(Right Panel)** Cell culture model experimental endpoint results. Results of qPCR are shown. $n = 3$. Statistical significance was determined by ANOVA; ns = non-significant; * $p < 0.05$; ** $p < 0.01$. **(B)** Mouse model. Eyes of GPR158 KO mice or their wild-type (WT) littermates were treated by periocular injections of Dex-loaded nanoparticles (Dex-NPs) twice a week, and/or topical delivery of dexamethasone (Dex) eye drops, 3 times per day, for 5–9 weeks. IOP was measured at the end of each week. In some experiments, IOP was also measured one week after Dex treatment was discontinued (After). **(Left Panel)** Dex-NPs treatment. **(Middle Panel)** Dex eye drop treatment. **(Right Panel)** Dex-NPs and Dex eye drop treatment. For all groups, $n = 6$; significance of IOP difference between KO and WT at each time point was tested by two-way ANOVA, with post hoc Bonferroni test. The adjusted p -value for the significant point in the left panel (at time point 3) is 0.0203.

2.4. Upstream GPCR Regulator *ADRB1* and Other Genes Linked to GPCR Signaling

As noted in the Introduction, we previously showed that the IOP-lowering effect of epinephrine, which signals via adrenergic receptors, was negated in *Gpr158* KO mice. This led to our interest in one final IPA-identified upstream regulator, the beta-adrenergic receptor *ADRB1*. The IPA predicted the pathway regulated by *ADRB1* to be affected by *GPR158* overexpression at $p = 3.87 \times 10^{-7}$.

We also identified individual genes regulated by GPR158 overexpression that are linked to both GPR158 signaling specifically, and GPCR signaling in general. These are listed in Table 5. *GNB5*, encoding the unconventional G protein that serves as the obligate

partner of the RGS7 GTPase, was upregulated. GPR158 recruits RGS7 to the plasma membrane via binding of GNB5, thus placing it in position to interact with GPCRs that bind conventional heterotrimeric G proteins of the Galpha (i/o) family to attenuate their signaling [44]. The upregulated *GNG7* encodes a G protein of the Galpha (i/o) family. *GNG7* has been shown to interact with GNB5 [65]. *RGS7* was expressed by TM-1 cells, but its expression level was not changed by GPR158 overexpression. However, *RGS4*, another GTPase, was one of the top downregulated genes (Table S1).

Table 5. GPR158-regulated genes involved in GPR158 and other GPCR signaling.

Gene	Fold Change in Gene Expression			Function
	Exp 1 Low, 72 h	Exp 2A High, 24 h	Exp 2B High, 96 h	
GPCR signaling				
<i>GNB5</i>			+1.281	G protein
<i>GNG7</i>		+1.360	+1.26	G protein
<i>RGS4</i>		−2.778	−2.21	GTPase activating
<i>PLCG1</i>			−1.387	Phospholipase C
<i>PLCH2</i>	+1.265			Phospholipase C

Shown are differentially expressed genes with the fold change in gene expression (+ or −) in each of the experiments. If a table cell is gray, the change in gene expression was not statistically significant.

Additionally changed in expression were two phospholipase C genes, the protein products of which are activated by G proteins to generate the second messenger inositol 1,4,5-trisphosphate. *PLCH2* was one of the top upregulated genes and *PLCG1* was one of the top downregulated genes (Table S1).

These findings identify genes affected by GPR158 overexpression that might take part in homeostatic IOP regulation.

3. Discussion

Physiological homeostasis is maintained through a fine regulation of the many steps involved in the function of neuroendocrine axes. The hypothalamic–pituitary–adrenal axis is activated by stress, leading to a production of glucocorticoid stress hormones by the adrenal glands, as well as the more rapidly acting catecholamine stress hormones, such as epinephrine. Epinephrine reduces IOP, but glucocorticoids can cause ocular hypertension in susceptible individuals [38]. The pathophysiology of ocular hypertension has also been linked to cellular stress responses including fibrosis [22–27], calcification [28], and UPR activation [29–34]. In a previous pharmacogenomic screen for genes associated with risk for ocular hypertension due to treatment with pharmacologic forms of glucocorticoids in the eye, we identified the novel GPCR, GPR158 [38,39].

GPR158 is most highly expressed in neuronal cells, including in the brain [40,66–69], in the retina of the eye [40,70], and in prostate cancer cells that have undergone neuroendocrine differentiation [41]. However, the gene is also expressed at lower levels in non-neuronal tissues, including prostate cancer epithelial cells [41] and the trabecular meshwork cells of the eye's aqueous outflow pathways [40]. We previously found that treatment with glucocorticoids induces expression of *GPR158* in prostate cancer [41] and trabecular meshwork cells in culture [39]. Significantly, *GPR158* overexpression increased survival of trabecular meshwork cells subjected to oxidative stress [39], a type of stress linked to the pathophysiology of POAG. Conversely, lack of *Gpr158* in knockout (KO) mice conferred protection against the elevation of IOP that occurred (in the C57Bl/6 inbred strain of mice used) as they aged [40]. These studies suggested that GPR158 can have both protective and pathological effects on the trabecular meshwork, thus, impacting development of ocular hypertension.

To identify pathways regulated by *GPR158* overexpression in trabecular meshwork cells, we performed microarray profiling of gene expression changes due to *GPR158* overexpression, then conducted pathway analysis. We identified four upstream stress regulators

relevant to ocular hypertension: dexamethasone, TGFB1, and the UPR components ATF4 and XPB1. Key genes in these pathways were downregulated by *GPR158* overexpression suggesting mechanisms that might confer the previously observed cytoprotection. Elevated IOP leading to both POAG and SIOH has been linked to fibrosis in the trabecular meshwork [2–4,6,13–21], as regulated by TGFB2 [22–27]. In turn, fibrosis has been linked to UPR activation [29–34]. ER stress occurs when protein folding capacity is compromised, either by an excessive load of translated proteins or a defect in molecular chaperones. The cell responds by activation of the UPR, a complex cellular process that alleviates the protein load of the ER, while increasing the expression of molecular chaperones, thus protecting cells (reviewed in [61,62]). A similar mechanism may be responsible for UPR activation by *GPR158* overexpression. GPCRs are integral membrane proteins that traverse the plasma membrane seven times. This structure makes the folding of GPCRs in the ER difficult and complex. Indeed, many wild-type GPCRs are not folded optimally, and defects in folding are the most common cause of genetic diseases due to GPCR mutations [71]. Depending on the acute or chronic nature of the stress, UPR activation might be cytoprotective or it might lead to cell death.

A fifth upstream stress regulator, TP53, was also identified. TP53 is a tumor suppressor that arrests cell replication by holding the cell cycle at the G1/S regulation point, when activated by a variety of cell stresses, through its action as a transcription factor [45]. The set of *GPR158*-regulated genes linked to TP53 was of interest because of our prior observations on the effects of *GPR158* on cell proliferation. We previously showed that dexamethasone treatment stimulates *GPR158* expression in trabecular meshwork cells. In turn, transient transfection with a *GPR158* expression vector also stimulates cell proliferation. Conversely, knockdown of endogenously expressed *GPR158* inhibits cell proliferation [39]. Similar effects of *GPR158* on cell proliferation were demonstrated in prostate cancer cell lines [41]; however, high-dose *GPR158*, as delivered via a doxycycline-inducible system similar to the one used in the current study, reverses this [41]. Our findings are consistent with the idea that activation of the TP53 pathway is responsible for the observed inhibition of cell proliferation at high doses of *GPR158* [41].

Activation of TP53 can occur in response to a number of cellular stresses, including DNA damage [72]. Under normal conditions, the TP53 level is maintained at a low state by virtue of the extremely short half-life of the polypeptide. Activation of TP53 in response to DNA damage is associated with a rapid increase in its level. Functioning as a transcription factor, TP53 then transactivates a number of genes whose products trigger cell-cycle arrest, apoptosis, or DNA repair. When damage is not too severe, the cell cycle pause provides cells an opportunity to repair themselves; however, when damage is severe, cell death programs are activated [73].

We previously showed that, once newly synthesized by cultured cells, *GPR158* traffics to the plasma membrane similar to other GPCRs; however, it is then rapidly endocytosed and translocates to the nucleus [39]. Mutation of the nuclear localization signal abrogates the enhancement of cell proliferation in both trabecular meshwork cells [39] and prostate cancer cell lines [41]. We conjecture that, when present at high doses, *GPR158* in the nucleus can cause DNA damage, thus activating the TP53 pathway. As with UPR activation, this would be expected to have a protective effect on cell survival if the damage is not too severe or prolonged.

Identification of these stress pathways was encouraging, but we found that the effect of changing pathway activity by *GPR158* overexpression is small. *GPR158* overexpression did not significantly inhibit the fibrotic response to dexamethasone, or affect calcification, and loss of *Gpr158* in KO mice only minimally protected against SIOH. The latter results contrast with our previous finding that lack of *Gpr158* in KO mice conferred protection against the elevation of IOP that occurred as mice aged [40]. One possible explanation for this different result is that the SIOH model is an acute stress, but the aging model is a chronic stress, with more time for effects of *GPR158* to manifest.

The sixth upstream regulator, *ADRB1*, may be the most significant. *ADRB1* is a beta adrenergic receptor subtype of GPCR family A. Drugs that enhance alpha adrenergic receptor activity (alpha agonists) or antagonize beta adrenergic receptor activity (beta blockers) are used clinically to lower IOP (reviewed in [74]). The acute stress hormone, epinephrine, is one of these drugs [75,76]. Epinephrine exerts its IOP-lowering effect through *ADRA2A*, which couples with $G_{\alpha}(s)$ to stimulate adenylyl cyclase and cAMP accumulation [77–81]. Trabecular meshwork cells also express *ADRB2*, which couples with $G_{\alpha}(i/o)$ to inhibit adenylyl cyclase; however, the positive IOP-lowering effect of *ADRA2A* activity appears to dominate [77–81].

GPR158 interacts with conventional GPCRs that bind G proteins of the $G_{\alpha}(i/o)$ class, such as beta adrenergic receptors, accelerating their deactivation via *RGS7* to enhance cAMP production [44]. Consistent with these mechanisms, we showed that *GPR158* overexpression in cultured trabecular meshwork cells enhanced cAMP accumulation in response to epinephrine and the IOP-lowering effect of epinephrine was negated in *Gpr158* KO mice [40]. These results suggest that adrenergic receptors partner with *GPR158* to maintain IOP homeostasis. Significantly, we also found several genes were regulated by *GPR158* overexpression encoding proteins of the envisioned partnership between the beta-adrenergic receptor and *GPR158*.

Additionally changed in response to *GPR158* overexpression was expression of two genes encoding different phospholipase C isoforms: *PLCH2* and *PLCG1*. *PLCG1* was one of the top downregulated genes, and *PLCH2* was one of the top upregulated genes. Phospholipase C is activated by G proteins of the $G_{q/11}$ family to generate the second messenger inositol 1,4,5-trisphosphate. This is intriguing in view of evidence suggesting that *GPR158* serves as a conventional GPCR receptor for *BGLAP*, a protein hormone that regulates bone remodeling and energy metabolism [69]. Biotin-labeled *BGLAP* bound a complex containing *Gpr158* and G_{q} . Consistent with the presence of G_{q} in this complex, *BGLAP* increased the production of inositol 1,4,5-trisphosphate significantly more in wild-type than hippocampal neurons from *Gpr158* KO mice and failed to increase in cAMP production. It has been shown that *BGLAP* is expressed by trabecular meshwork cells [28]; we confirmed this here, but found the level was unchanged by *GPR158* overexpression. *PLCH2* has been previously shown to be highly expressed in neuronal cells of the brain [82,83] and the retina [84,85]. Future studies will be needed to determine whether *PLCH2* plays a role in *GPR158* signaling.

In summary, we identified five upstream stress regulators that control gene sets modulated by *GPR158* overexpression, and we argue that regulation of each of these pathways might contribute in some small way to the previously observed effects of *GPR158* on ocular hypertension. Potentially of greater significance, we report new evidence to support previous findings that *GPR158* modulates adrenergic receptor signaling, essential to the homeostatic maintenance of IOP. This and the *GPR158* and GPCR pathway genes identified as differentially regulated by *GPR158* warrant follow-up in future studies. Very recently, *GPR158* was deorphanized [86]. It was found that the amino acid glycine directly binds to a Cache domain of *GPR158*, and this inhibits the activity of the associated *RGS7-GB5*, inhibiting production of cAMP. The two systems likely overlap and are involved in autotuning and homeostatic feedback. Identification of an activating ligand provides an opportunity for development of drugs that target *GPR158* to control IOP in glaucoma.

4. Materials and Methods

4.1. Antibodies

Primary antibodies used for immunolocalization or immunoblotting are shown in Table 6. The antibody specific for human *GPR158* was raised against AAs 24–74 of the human *GPR158* extracellular domain. Its use for immunohistochemistry, immunolocalization and immunoblot analysis in human and mouse cells and tissues has been described in several publications from our labs [39,41,44,70,87].

Table 6. Primary antibodies used for immunolocalization and immunoblotting.

Antigen	Where Purchased	Catalogue Number	Species
GPR158	Sigma-Aldrich Corporation, St Louis, MO, USA	Cat# HPA013185	Rabbit
MYOC	Santa Cruz Biotechnology, Santa Cruz, CA, USA	Cat# sc-137233	Mouse
TP53	Cell Signaling Technology, Danvers, MA, USA	Cat# IC12	Mouse
COL10A1	Invitrogen, Waltham, MA, USA	Cat# PA5-49198	Rabbit
SLCA8	Origene Technologies, Rockville, MD, USA	Cat# TA328916	Rabbit
HSPA5 (GRP78/BiP)	Abcam, Cambridge, UK	Cat# ab212054	Mouse
ATF4	Cell Signaling Technology, Danvers, MA, USA	Cat# 11815	Rabbit
DDIT3 (CHOP)	Cell Signaling Technology, Danvers, MA, USA	Cat# 5554	Rabbit
ACTB	Abcam, Cambridge, UK	Cat# ab6276	Mouse
GAPDH	Cell Signaling Technology, Danvers, MA, USA	Cat# 97166	Mouse

4.2. Immortalized Trabecular Meshwork Cell Line and Lentivirus-Transformed GPR158 Overexpression Model

An SV40 large T-antigen immortalized human trabecular meshwork cell line, TM-1 [88], was generously donated by Dr. Donna Peters (University of Wisconsin, Madison, WI, USA). The line was created in the laboratory of the late Dr. Jon Polansky from trabecular meshwork cells obtained from a 30-year-old non-glaucomatous individual, as previously described [88]. The original parental trabecular meshwork cells were characterized as previously described [89,90] and shown along with the TM-1 cells to upregulate MYOC in response to dexamethasone [88,91]. Cells were grown in low-glucose Dulbecco's modified Eagle's medium containing 10% FBS (Atlanta Biologicals, Inc., Norcross, GA, USA), 2 mM L-glutamine, 2.5 ug/mL amphotericin B, and 25 ug/mL gentamicin, as previously described [88].

To create the inducible *GPR158* overexpression model, TM-1 cells were transduced with a lentiviral vector containing *GPR158*, in which expression is driven by a doxycycline-inducible promoter (pSlik-Hygro, Addgene, Cambridge, MA, USA), as previously described [41]. A stably transduced cell line was selected and named lenti-GPR158 TM-1. *GPR158* transgene expression is leaky, thus the lenti-GPR158 TM-1 cell line, untreated with doxycycline, is not a perfect negative control. For this reason, a matching negative control cell line, stably transduced with empty vector, was also created and named lenti-vector TM-1.

4.3. Human Trabecular Meshwork Primary Cell Strains and Transient Transfection

Primary human TM cells were used for validation of data obtained with the immortalized TM-1 cell line. Cells were isolated from whole eyes that were obtained from Miracles in Sight Eye Bank (Winston Salem, NC, USA) and distributed to us by BioSight Biorepository at Duke University under exempt IRB #113746. Primary cell strain TM137 was from a 60 years old white male donor; primary cell strain TM200 was from a 68 years old white female donor. Neither donor eye was glaucomatous. Cells were isolated, characterized and cultured as described [92,93], according to consensus guidelines [94]. Cells were cultured in low-glucose Dulbecco's modified Eagle's medium containing 10% FBS (Gibco BRL, New York, NY, USA), 2 mM L-glutamine, 2.5 ug/mL amphotericin B, and 25 ug/mL gentamicin, as described [88]. Cells between passages 5 and 7, were transiently transfected with a

GPR158 expression construct, previously described [39], or empty vector (control) for 48 h using Lipofectamine 3000 Transfection Reagent (Life Technologies, Grand Island, NY, USA).

4.4. Microarray-Based Gene Expression Profiling

For induction of GPR158 expression, cells of the lenti-GPR158 TM-1 cell line and lenti-vector TM-1 cell line were seeded at 10^5 /mL in the wells of 6-well plates. Cells were maintained in reduced serum (2.5%) for the experimental time periods. Two experiments were performed. In the first experiment, cells were treated with doxycycline at 100 ng/mL for 72 h ($n = 3$). A parallel set of lenti-vector cell cultures was also left untreated for the same period as a negative control. In the second experiment, cells were treated with doxycycline at 500 ng/mL for 24 h or 96 h ($n = 3$), also using the lenti-vector cell line as a negative control. We have previously described use of the 100 ng/mL and 500 ng/mL treatments in a similar lentiviral-transformed prostate cancer cell model [41]. In each experiment, GPR158 induction was quantified for each GPR158 dose by immunoblotting.

Total RNA was extracted from each culture plate well using Aurum (Bio-Rad, Hercules, CA, USA) quantified by Nanodrop (ND-1000, Thermo Scientific Inc., Rockford, IL, USA), and sent to the UCLA Neuroscience Core (Los Angeles, CA, USA) for gene expression microarray screening. Gene expression profiling on each individual sample was performed using the BeadChip™ platform (Illumina, San Diego, CA, USA) Human HT-12 v4.0. Cyanine-3-labelled cRNA was hybridized on Agilent SurePrint G3 Human GE 8 × 60K Microarray v2. Arrays were scanned with an Agilent DNA Microarray Scanner at a 3- μ m scan resolution, image data were processed with Agilent Feature Extraction 11.0.1.1, and processed signals were quantile normalized with Agilent GeneSpring 12.0.

Quantile normalized intensities were imported into Partek® Genomics Suite® software, version 6.6 Copyright ©; 2016 (Partek Inc., St. Louis, MO, USA) for differential expression analysis. The normalized expression intensities for all probes were subjected to a two-way analysis of variance analysis (ANOVA, San Francisco, CA, USA). Differentially expressed genes were selected using criteria p-value (or FDR using the Benjamini–Hochberg method) <0.05 and fold change ≥ 1.2 .

4.5. Ingenuity Pathway Analysis

Pathway analysis was performed using Ingenuity Pathway Analysis (IPA) software (Qiagen, Mountain View, CA, USA; <http://www.ingenuity.com> accessed on 18 July 2023) to identify biological functions and disease categories that are enriched among the differentially expressed genes identified by microarray. The IPA upstream regulator tool was used to predict signal transduction pathways affected.

4.6. Quantitative Polymerase Chain Reaction (qPCR)

For gene expression analysis, RNA was isolated using GeneJET RNA Purification Kit (Thermo Fisher Scientific) following the manufacturer's instructions. DNA contamination was removed from columns with PureLink® DNase Set (Invitrogen, Carlsbad, CA, USA). Reverse transcription was performed with High Capacity Reverse Transcription Kit (Applied Biosystems, Foster City, CA, USA) to synthesize the first-strand cDNA from 1 μ g of total RNA.

The qPCR reaction was performed using SYBR® Green reagents (iQaq Universal SYBR Green Supermix; Bio-Rad, Hercules, CA, USA) with specific primers (Table 7). The following parameters were used: 30 s at 95 °C, followed by 40 cycles of 5 s at 95 °C and 30 s at 60 °C. All samples were normalized to RNA levels of the housekeeping gene *ACTB* (Table 7). The comparative CT method was used for relative quantitation [95], selecting the relative amount in control cells as the calibrator.

Table 7. Primer sequences for qPCR.

Gene	Primer Sequence
<i>TGFB2</i>	Forward: GCGACGAAGAGTACTACGCC Reverse: TGGCATCAAGGTACCCACAG
<i>COL10A1</i>	Forward: CAAGGCACCATCTCCAGG AA Reverse: AAAGGGTAT TTGTGGCAGCATATT
<i>CA12</i>	Forward: ACTGCGGCAGGACTGAGTCT Reverse: CACAATACAGATGCCAAGAATGC
<i>TP53</i>	Forward: TTTTCCCCTCCCATGTGCTC Reverse: TGGACGGTGGCTCTAGACTT
<i>FN1</i>	Forward: AGCGGACCTACCTAGGCAAT Reverse: GGTTTGCGATGGTACAGCTT
<i>HSPA5</i>	Forward: CCAAGAGAGGGTCTTGAATCTCG Reverse: ATGGGCCAGCCTGGATATAACA
<i>sXBP1</i>	Forward: CTGAGTCCGAATCAGGTGCAG Reverse: ATCCATGGGGAGATGTTCTGG
<i>ATF4</i>	Forward: CAGCACAGCCCCCTTACCA Reverse: GCCCGCCTTAGCCTTGTC
<i>DDIT3</i>	Forward: AGAACCAGGAAACGGAAACAGA Reverse: TCTCCTTCATGCGCTGCTTT
<i>ACTB</i>	Forward: GTCATTCCAAATATGAGATGCGT Reverse: GCTATCACCTCCCCTGTGTG

4.7. Immunoblotting

Cells were lysed by suspension in 200 μ L of RIPA (radioimmunoprecipitation assay) lysis buffer containing Tris 50 mM, NaCl 150 mM, SDS 0.1%, sodium deoxycholate 0.5%, NP-40 1% and protease inhibitors cocktail. After 20 min, the lysates were centrifuged at $10,000 \times g$ for 10 min and supernatants were collected. Proteins in the extracts were separated by SDS-PAGE. Samples were prepared without boiling (which causes aggregation of GPR158); however, samples were reduced with beta-mercaptoethanol. Equal protein was loaded into each well based on bicinchoninic acid (BCA) assay (Thermo Scientific, Rockford, IL, USA).

Proteins separated by SDS-PAGE were transferred to polyvinylidene difluoride (PVDF) membranes. Membranes were probed with primary antibody overnight at 4 °C with gentle shaking, following the manufacturer's instructions. Protein loading equivalence was monitored by probing of the membrane with antibody to the housekeeping gene ACTB. All the primary antibodies for immunoblot analysis were used at 1:1000 dilution, except ACTB, which was used at 1:4000 dilution.

Following incubation with primary antibodies, the membranes were then incubated for 1 h with secondary antibody–horseradish peroxidase conjugates (Santa Cruz Biotechnology, Santa Cruz, CA, USA) at a dilution of 1:10,000. Specific signals were developed for 1 min using the enhanced chemiluminescence (ECL) kit components 1 and 2 (GE Healthcare UK Limited, Buckinghamshire, UK). Chemiluminescence was visualized by exposure of photographic film (LAS-4000; Fujifilm, Tokyo, Japan).

4.8. Calcification Assay

Transgene expression in lenti-GPR158 TM-1 cells was induced by treatment with doxycycline at 100 or 500 ng/mL for 3-5 days. Alizarin red staining for calcification was then performed according to a published method previously used to detect calcification in cultured trabecular meshwork cells treated with dexamethasone [96]. Briefly, cells were fixed in cold 100% methanol, then washed and exposed to fresh 1.5% alizarin red (pH 4.2; Sigma-Aldrich, St. Louis, MO, USA) for 5 min (red-orange shows positive staining). Subsequently, cells were washed again and photographed with a microscope-mounted digital camera (Nikon Eclipse Nikon, Melville, NY, USA).

4.9. Mouse Model of Steroid-Induced Ocular Hypertension

All studies were carried out in accordance with the Association for Research in Vision and Ophthalmology (ARVO, Rockville, MD, USA) statement for the Use of Animals in Ophthalmic and Vision Research and the recommendations of the NIH Guide for the Care and Use of Laboratory Animals. All procedures were approved by the Institutional Animal Care and Use Committee of Tufts University/Tufts Medical Center (protocol number B2019-39).

Gpr158 KO mice (*Gpr158^{tm1(KOMP)Vlcg}*) were originally purchased from the University of California Davis Knockout Mouse Project (KOMP) Repository. Data on the KOMP website indicate that homozygotes for the KO allele are viable and anatomically normal. Mice were backcrossed onto the C57/Bl6J background for at least 4 generations at The Scripps Research Institute (Jupiter, FL, USA). Heterozygous *Gpr158*^{-/+} pairs were imported to Tufts Medical Center (Boston, MA, USA), then bred to generate sufficient homozygous knockout mice (*Gpr158*^{-/-}) and wild-type littermates (*Gpr158*^{+/+}) for experiments. Littermates were used exclusively for all comparisons. Males were also used exclusively because glucocorticoid treatment exhibits sex-specific differences [97]. Mice were housed on a 12-h light–dark cycle with food and water available ad libitum.

In humans, there is considerable inter-individual variability in glucocorticoid response [38]; however, mice bred onto the inbred C57Bl/6 background uniformly develop ocular hypertension when treated with glucocorticoids (e.g., [33]). To create glucocorticoid-induced ocular hypertension, dexamethasone was delivered to eyes of 4–6 month old mice in three different ways: (1) as eye drops, (2) as loaded nanoparticles (Dex-NPs), (3) as both eye drops and nanoparticles.

For eye drop delivery, dexamethasone phosphate (0.1% in PBS) or vehicle (~20 µL) were delivered 3 times per day, as previously described [33]. For nanoparticle delivery, Dex-NPs (containing ~23 µg of dexamethasone) or unloaded NPs were injected periorbitally, 2 times per week, as previously described [98]. Dexamethasone delivery was performed for 5–9 weeks.

Intraocular pressure measurement was performed in anesthetized mice by rebound tonometry using the TonoLab (Icare, Revenio Group, Vantaa, Finland) [99]. Each recorded IOP was the average of six measurements, giving a total of 36 rebounds from the same eye per recorded intraocular pressure value. IOP was measured at the end of each week. In some experiments, IOP was also measured one week after dexamethasone treatment was discontinued.

4.10. Statistical Analysis and Reproducibility

All experiments were repeated at least twice, and usually three times. All cells, tissues, and animals were randomly assigned to the experimental groups. All data are shown as the means ± standard deviation (SD). For the calculation of *p* values, all technical replicates from all biological replicates were used. All cell culture assays were performed with at least *n* = 3 biological replicates. The number of animals needed per experimental group was estimated as *n* = 6 biological replicates. Statistical analysis was performed using GraphPad Prism 7 (GraphPad Software, San Diego, CA, USA). The Student *t*-test or the Mann–Whitney U test was used attending to normality of the data distribution as determined by using the D’Agostino and Pearson normality test. Analysis of Variance (ANOVA, San Francisco, CA, USA) with Bonferroni’s post hoc test was applied for comparison of multiple samples. A *p*-value ≥ 0.05 was treated as significant.

Supplementary Materials: The following supporting information can be downloaded at: <https://www.mdpi.com/article/10.3390/stresses3030044/s1>, Table S1: Top genes upregulated or downregulated by GPR158 overexpression.

Author Contributions: Conceptualization, M.F.S., T.I. and M.E.F.; data curation, J.E. and H.M.S.; formal analysis, T.I. and M.E.F.; funding acquisition, W.D.S. and M.E.F.; investigation, M.F.S., T.I., S.P., S.J. and S.K.C.; methodology, M.F.S., T.I., S.P., S.J., S.K.C., S.R., T.L., W.D.S. and M.E.F.; project administration, S.P. and M.E.F.; resources, M.B.R., S.R., T.L. and W.D.S.; supervision, M.E.F.; validation, M.F.S.; writing—original draft, M.F.S., T.I. and M.E.F.; writing—review and editing, M.F.S., T.I., S.P., S.J., S.K.C., M.B.R., S.R., T.L., J.E., H.M.S., W.D.S. and M.E.F. All authors have read and agreed to the published version of the manuscript.

Funding: This research was funded by NIH grants R01EY027315 (to MEF) and R01EY030124 (to WDS), an unrestricted challenge grant from Research to Prevent Blindness, and a grant from the Massachusetts Lions Eye Research Fund. The Integrated Molecular Technologies Core is supported by NIH center grant P30DK041301 to the UCLA CURE: Digestive Diseases Research Center.

Data Availability Statement: The microarray data from this study have been deposited in the Gene Expression Omnibus (GEO) data repository, of the National Center for Biotechnology Information, U.S. National Library of Medicine, Bethesda, MD, USA with accession numbers GSM7516818 to GSM7516853. All other data is contained within this paper.

Acknowledgments: The authors thank the USC Department of Pathology's Immunohistochemistry Laboratory for technical assistance with the immunohistochemical studies, the University of California Los Angeles (UCLA) Neuroscience Genomics Core for microarray-based gene expression services, and the UCLA Integrated Molecular Technologies Core/Vector Core for lentiviral production. Yibu Chen of the USC Libraries Bioinformatics Service is gratefully acknowledged for assistance with the gene expression data analysis. Stefanie Gavett, Jocelyn Munguia and Quinn Goble of the Tufts Comparative Medicine Services Rodent Breeding Service are gratefully acknowledged for management of the mouse breeding colony. The telomerase immortalized human trabecular meshwork cell line, TM-1, was generously donated by Donna Peters, University of Wisconsin-Madison, and the Gpr158 knockout mice were a kind gift of Kirill Martemyanov of the Scripps Research Institute, Jupiter, FL. The Mouse Biology Program (www.mousebiology.org) at the University of California Davis is gratefully acknowledged for providing the original line of Gpr158 KO mice. Rafael Martinez-Carrasco is gratefully acknowledged for assistance with graphics.

Conflicts of Interest: The authors declare no conflict of interest. The funders had no role in the design of the study; in the collection, analyses, or interpretation of data; in the writing of the manuscript; or in the decision to publish the results.

References

1. Sharif, N.A. Therapeutic Drugs and Devices for Tackling Ocular Hypertension and Glaucoma, and Need for Neuroprotection and Cytoprotective Therapies. *Front. Pharmacol.* **2021**, *12*, 729249. [[CrossRef](#)] [[PubMed](#)]
2. Epstein, D.L.; Allingham, R.R.; Schuman, J.S. *Chandler and Grant's Glaucoma*, 4th ed.; Williams and Wilkins: Baltimore, Maryland, 1996.
3. Grant, W.M. Experimental aqueous perfusion in enucleated human eyes. *Arch. Ophthalmol.* **1963**, *69*, 783–801. [[CrossRef](#)] [[PubMed](#)]
4. Alvarado, J.; Murphy, C.; Polansky, J.; Juster, R. Age-related changes in trabecular meshwork cellularity. *Investig. Ophthalmol. Vis. Sci.* **1981**, *21*, 714–727.
5. Alvarado, J.A.; Wood, I.; Polansky, J.R. Human trabecular cells. II. Growth pattern and ultrastructural characteristics. *Investig. Ophthalmol. Vis. Sci.* **1982**, *23*, 464–478.
6. Alvarado, J.; Murphy, C.; Juster, R. Trabecular meshwork cellularity in primary open-angle glaucoma and nonglaucomatous normals. *Ophthalmology* **1984**, *91*, 564–579. [[CrossRef](#)]
7. Alvarado, J.A.; Alvarado, R.G.; Yeh, R.F.; Franse-Carman, L.; Marcellino, G.R.; Brownstein, M.J. A new insight into the cellular regulation of aqueous outflow: How trabecular meshwork endothelial cells drive a mechanism that regulates the permeability of Schlemm's canal endothelial cells. *Br. J. Ophthalmol.* **2005**, *89*, 1500–1505. [[CrossRef](#)]
8. Adams, C.M.; Stacy, R.; Rangaswamy, N.; Bigelow, C.; Grosskreutz, C.L.; Prasanna, G. Glaucoma—Next Generation Therapeutics: Impossible to Possible. *Pharm. Res.* **2018**, *36*, 25. [[CrossRef](#)] [[PubMed](#)]
9. Acott, T.S.; Kelley, M.J. Extracellular matrix in the trabecular meshwork. *Exp. Eye Res.* **2008**, *86*, 543–561. [[CrossRef](#)]
10. Ethier, C.R. The inner wall of Schlemm's canal. *Exp. Eye Res.* **2002**, *74*, 161–172. [[CrossRef](#)]
11. Johnson, M. What controls aqueous humour outflow resistance? *Exp. Eye Res.* **2006**, *82*, 545–557. [[CrossRef](#)]
12. Maepea, O.; Bill, A. Pressures in the juxtacanalicular tissue and Schlemm's canal in monkeys. *Exp. Eye Res.* **1992**, *54*, 879–883. [[CrossRef](#)]

13. Lutjen-Drecoll, E.; Shimizu, T.; Rohrbach, M.; Rohen, J.W. Quantitative analysis of 'plaque material' in the inner- and outer wall of Schlemm's canal in normal- and glaucomatous eyes. *Exp. Eye Res.* **1986**, *42*, 443–455. [[CrossRef](#)]
14. Schuman, J.S.; Wang, N.; Eisenberg, D.L. Leukemic glaucoma: The effects on outflow facility of chronic lymphocytic leukemia lymphocytes. *Exp. Eye Res.* **1995**, *61*, 609–617. [[CrossRef](#)]
15. Underwood, J.L.; Murphy, C.G.; Chen, J.; Franse-Carman, L.; Wood, I.; Epstein, D.L.; Alvarado, J.A. Glucocorticoids regulate transendothelial fluid flow resistance and formation of intercellular junctions. *Am. J. Physiol.* **1999**, *277*, C330–C342. [[CrossRef](#)]
16. Tripathi, R.C. Mechanism of the aqueous outflow across the trabecular wall of Schlemm's canal. *Exp. Eye Res.* **1971**, *11*, 116–121. [[CrossRef](#)] [[PubMed](#)]
17. Vranka, J.A.; Kelley, M.J.; Acott, T.S.; Keller, K.E. Extracellular matrix in the trabecular meshwork: Intraocular pressure regulation and dysregulation in glaucoma. *Exp. Eye Res.* **2015**, *133*, 112–125. [[CrossRef](#)] [[PubMed](#)]
18. Stamer, W.D.; Braakman, S.T.; Zhou, E.H.; Ethier, C.R.; Fredberg, J.J.; Overby, D.R.; Johnson, M. Biomechanics of Schlemm's canal endothelium and intraocular pressure reduction. *Prog. Retin. Eye Res.* **2015**, *44*, 86–98. [[CrossRef](#)] [[PubMed](#)]
19. Braunger, B.M.; Fuchshofer, R.; Tamm, E.R. The aqueous humor outflow pathways in glaucoma: A unifying concept of disease mechanisms and causative treatment. *Eur. J. Pharm. Biopharm.* **2015**, *95*, 173–181. [[CrossRef](#)]
20. Filla, M.S.; Faralli, J.A.; Peotter, J.L.; Peters, D.M. The role of integrins in glaucoma. *Exp. Eye Res.* **2016**. [[CrossRef](#)]
21. Gagen, D.; Faralli, J.A.; Filla, M.S.; Peters, D.M. The role of integrins in the trabecular meshwork. *J. Ocul. Pharmacol. Ther.* **2014**, *30*, 110–120. [[CrossRef](#)]
22. Lutjen-Drecoll, E. Morphological changes in glaucomatous eyes and the role of TGFbeta2 for the pathogenesis of the disease. *Exp. Eye Res.* **2005**, *81*, 1–4. [[CrossRef](#)]
23. Shepard, A.R.; Millar, J.C.; Pang, I.H.; Jacobson, N.; Wang, W.H.; Clark, A.F. Adenoviral gene transfer of active human transforming growth factor- β 2 elevates intraocular pressure and reduces outflow facility in rodent eyes. *Investig. Ophthalmol. Vis. Sci.* **2010**, *51*, 2067–2076. [[CrossRef](#)]
24. Wordinger, R.J.; Fleenor, D.L.; Hellberg, P.E.; Pang, I.H.; Tovar, T.O.; Zode, G.S.; Fuller, J.A.; Clark, A.F. Effects of TGF- β 2, BMP-4, and gremlin in the trabecular meshwork: Implications for glaucoma. *Investig. Ophthalmol. Vis. Sci.* **2007**, *48*, 1191–1200. [[CrossRef](#)]
25. Zode, G.S.; Clark, A.F.; Wordinger, R.J. Bone morphogenetic protein 4 inhibits TGF- β 2 stimulation of extracellular matrix proteins in optic nerve head cells: Role of gremlin in ECM modulation. *Glia* **2009**, *57*, 755–766. [[CrossRef](#)] [[PubMed](#)]
26. Wang, W.H.; McNatt, L.G.; Pang, I.H.; Millar, J.C.; Hellberg, P.E.; Hellberg, M.H.; Steely, H.T.; Rubin, J.S.; Fingert, J.H.; Sheffield, V.C.; et al. Increased expression of the WNT antagonist sFRP-1 in glaucoma elevates intraocular pressure. *J. Clin. Investig.* **2008**, *118*, 1056–1064. [[CrossRef](#)] [[PubMed](#)]
27. Mao, W.; Millar, J.C.; Wang, W.H.; Silverman, S.M.; Liu, Y.; Wordinger, R.J.; Rubin, J.S.; Pang, I.H.; Clark, A.F. Existence of the canonical Wnt signaling pathway in the human trabecular meshwork. *Investig. Ophthalmol. Vis. Sci.* **2012**, *53*, 7043–7051. [[CrossRef](#)] [[PubMed](#)]
28. Borrás, T.; Comes, N. Evidence for a calcification process in the trabecular meshwork. *Exp. Eye Res.* **2009**, *88*, 738–746. [[CrossRef](#)]
29. Peters, J.C.; Bhattacharya, S.; Clark, A.F.; Zode, G.S. Increased Endoplasmic Reticulum Stress in Human Glaucomatous Trabecular Meshwork Cells and Tissues. *Investig. Ophthalmol. Vis. Sci.* **2015**, *56*, 3860–3868. [[CrossRef](#)]
30. Zode, G.S.; Kuehn, M.H.; Nishimura, D.Y.; Searby, C.C.; Mohan, K.; Grozdanic, S.D.; Bugge, K.; Anderson, M.G.; Clark, A.F.; Stone, E.M.; et al. Reduction of ER stress via a chemical chaperone prevents disease phenotypes in a mouse model of primary open angle glaucoma. *J. Clin. Investig.* **2015**, *125*, 3303. [[CrossRef](#)] [[PubMed](#)]
31. Kasetti, R.B.; Maddineni, P.; Millar, J.C.; Clark, A.F.; Zode, G.S. Increased synthesis and deposition of extracellular matrix proteins leads to endoplasmic reticulum stress in the trabecular meshwork. *Sci. Rep.* **2017**, *7*, 14951. [[CrossRef](#)]
32. Kasetti, R.B.; Patel, P.D.; Maddineni, P.; Patil, S.; Kiehlbauch, C.; Millar, J.C.; Searby, C.C.; Raghunathan, V.; Sheffield, V.C.; Zode, G.S. ATF4 leads to glaucoma by promoting protein synthesis and ER client protein load. *Nat. Commun.* **2020**, *11*, 5594. [[CrossRef](#)] [[PubMed](#)]
33. Zode, G.S.; Sharma, A.B.; Lin, X.; Searby, C.C.; Bugge, K.; Kim, G.H.; Clark, A.F.; Sheffield, V.C. Ocular-specific ER stress reduction rescues glaucoma in murine glucocorticoid-induced glaucoma. *J. Clin. Investig.* **2014**, *124*, 1956–1965. [[CrossRef](#)] [[PubMed](#)]
34. Kasetti, R.B.; Maddineni, P.; Patel, P.D.; Searby, C.; Sheffield, V.C.; Zode, G.S. Transforming growth factor beta2 (TGFbeta2) signaling plays a key role in glucocorticoid-induced ocular hypertension. *J. Biol. Chem.* **2018**, *293*, 9854–9868. [[CrossRef](#)]
35. Iglesias, A.I.; Springelkamp, H.; Ramdas, W.D.; Klaver, C.C.; Willemsen, R.; van Duijn, C.M. Genes, pathways, and animal models in primary open-angle glaucoma. *Eye* **2015**, *29*, 1285–1298. [[CrossRef](#)] [[PubMed](#)]
36. Liu, Y.; Allingham, R.R. Major review: Molecular genetics of primary open-angle glaucoma. *Exp. Eye Res.* **2017**, *160*, 62–84. [[CrossRef](#)] [[PubMed](#)]
37. Gharahkhani, P.; Jorgenson, E.; Hysi, P.; Khawaja, A.P.; Pendergrass, S.; Han, X.; Ong, J.S.; Hewitt, A.W.; Segre, A.V.; Rouhana, J.M.; et al. Genome-wide meta-analysis identifies 127 open-angle glaucoma loci with consistent effect across ancestries. *Nat. Commun.* **2021**, *12*, 1258. [[CrossRef](#)]
38. Fini, M.E.; Schwartz, S.G.; Gao, X.; Jeong, S.; Patel, N.; Itakura, T.; Price, M.O.; Price, F.W., Jr.; Varma, R.; Stamer, W.D. Steroid-induced ocular hypertension/glaucoma: Focus on pharmacogenomics and implications for precision medicine. *Prog. Retin. Eye Res.* **2017**, *56*, 58–83. [[CrossRef](#)]

39. Patel, N.; Itakura, T.; Gonzalez, J.M., Jr.; Schwartz, S.G.; Fini, M.E. GPR158, an orphan member of G protein-coupled receptor Family C: Glucocorticoid-stimulated expression and novel nuclear role. *PLoS ONE* **2013**, *8*, e57843. [[CrossRef](#)] [[PubMed](#)]
40. Itakura, T.; Webster, A.; Chintala, S.K.; Wang, Y.; Gonzalez, J.M., Jr.; Tan, J.C.; Vranka, J.A.; Acott, T.; Craft, C.M.; Sibug Saber, M.E.; et al. GPR158 in the Visual System: Homeostatic Role in Regulation of Intraocular Pressure. *J. Ocul. Pharmacol. Ther.* **2019**, *35*, 203–215. [[CrossRef](#)] [[PubMed](#)]
41. Patel, N.; Itakura, T.; Jeong, S.; Liao, C.P.; Roy-Burman, P.; Zandi, E.; Groshen, S.; Pinski, J.; Coetzee, G.A.; Gross, M.E.; et al. Expression and Functional Role of Orphan Receptor GPR158 in Prostate Cancer Growth and Progression. *PLoS ONE* **2015**, *10*, e0117758. [[CrossRef](#)] [[PubMed](#)]
42. Levoye, A.; Dam, J.; Ayoub, M.A.; Guillaume, J.L.; Jockers, R. Do orphan G-protein-coupled receptors have ligand-independent functions? New insights from receptor heterodimers. *EMBO Rep.* **2006**, *7*, 1094–1098. [[CrossRef](#)] [[PubMed](#)]
43. Milligan, G. G protein-coupled receptor hetero-dimerization: Contribution to pharmacology and function. *Br. J. Pharmacol.* **2009**, *158*, 5–14. [[CrossRef](#)] [[PubMed](#)]
44. Orlandi, C.; Xie, K.; Masuho, I.; Fajardo-Serrano, A.; Lujan, R.; Martemyanov, K.A. Orphan Receptor GPR158 Is an Allosteric Modulator of RGS7 Catalytic Activity with an Essential Role in Dictating Its Expression and Localization in the Brain. *J. Biol. Chem.* **2015**, *290*, 13622–13639. [[CrossRef](#)] [[PubMed](#)]
45. Kruiswijk, F.; Labuschagne, C.F.; Vousden, K.H. p53 in survival, death and metabolic health: A lifeguard with a licence to kill. *Nat. Reviews. Mol. Cell Biol.* **2015**, *16*, 393–405. [[CrossRef](#)]
46. Byrns, M.C.; Jin, Y.; Penning, T.M. Inhibitors of type 5 β -hydroxysteroid dehydrogenase (AKR1C3): Overview and structural insights. *J. Steroid Biochem. Mol. Biol.* **2011**, *125*, 95–104. [[CrossRef](#)] [[PubMed](#)]
47. Liton, P.B.; Liu, X.; Stamer, W.D.; Challa, P.; Epstein, D.L.; Gonzalez, P. Specific targeting of gene expression to a subset of human trabecular meshwork cells using the chitinase 3-like 1 promoter. *Investig. Ophthalmol. Vis. Sci.* **2005**, *46*, 183–190. [[CrossRef](#)] [[PubMed](#)]
48. Liao, S.Y.; Ivanov, S.; Ivanova, A.; Ghosh, S.; Cote, M.A.; Keefe, K.; Coca-Prados, M.; Stanbridge, E.J.; Lerman, M.I. Expression of cell surface transmembrane carbonic anhydrase genes CA9 and CA12 in the human eye: Overexpression of CA12 (CAXII) in glaucoma. *J. Med. Genet* **2003**, *40*, 257–261. [[CrossRef](#)] [[PubMed](#)]
49. Lo, W.R.; Rowlette, L.L.; Caballero, M.; Yang, P.; Hernandez, M.R.; Borrás, T. Tissue differential microarray analysis of dexamethasone induction reveals potential mechanisms of steroid glaucoma. *Investig. Ophthalmol. Vis. Sci.* **2003**, *44*, 473–485. [[CrossRef](#)]
50. Rozsa, F.W.; Reed, D.M.; Scott, K.M.; Pawar, H.; Moroi, S.E.; Kijek, T.G.; Krafchak, C.M.; Othman, M.I.; Vollrath, D.; Elnér, V.M.; et al. Gene expression profile of human trabecular meshwork cells in response to long-term dexamethasone exposure. *Mol. Vis.* **2006**, *12*, 125–141. [[PubMed](#)]
51. Ishibashi, T.; Takagi, Y.; Mori, K.; Naruse, S.; Nishino, H.; Yue, B.Y.; Kinoshita, S. cDNA microarray analysis of gene expression changes induced by dexamethasone in cultured human trabecular meshwork cells. *Investig. Ophthalmol. Vis. Sci.* **2002**, *43*, 3691–3697.
52. Nehme, A.; Lobenhofer, E.K.; Stamer, W.D.; Edelman, J.L. Glucocorticoids with different chemical structures but similar glucocorticoid receptor potency regulate subsets of common and unique genes in human trabecular meshwork cells. *BMC Med. Genom.* **2009**, *2*, 58. [[CrossRef](#)]
53. Danias, J.; Gerometta, R.; Ge, Y.; Ren, L.; Panagis, L.; Mittag, T.W.; Candia, O.A.; Podos, S.M. Gene expression changes in steroid-induced IOP elevation in bovine trabecular meshwork. *Investig. Ophthalmol. Vis. Sci.* **2011**, *52*, 8636–8645. [[CrossRef](#)] [[PubMed](#)]
54. Keller, K.E.; Bradley, J.M.; Vranka, J.A.; Acott, T.S. Segmental versican expression in the trabecular meshwork and involvement in outflow facility. *Investig. Ophthalmol. Vis. Sci.* **2011**, *52*, 5049–5057. [[CrossRef](#)]
55. Picht, G.; Welge-Luessen, U.; Grehn, F.; Lutjen-Drecoll, E. Transforming growth factor beta 2 levels in the aqueous humor in different types of glaucoma and the relation to filtering bleb development. *Graefes. Arch Clin. Exp. Ophthalmol.* **2001**, *239*, 199–207. [[CrossRef](#)]
56. Tripathi, R.C.; Li, J.; Chan, W.F.; Tripathi, B.J. Aqueous humor in glaucomatous eyes contains an increased level of TGF-beta 2. *Exp. Eye Res.* **1994**, *59*, 723–727. [[CrossRef](#)]
57. Flugel-Koch, C.; Ohlmann, A.; Fuchshofer, R.; Welge-Lussen, U.; Tamm, E.R. Thrombospondin-1 in the trabecular meshwork: Localization in normal and glaucomatous eyes, and induction by TGF-beta1 and dexamethasone in vitro. *Exp. Eye Res.* **2004**, *79*, 649–663. [[CrossRef](#)] [[PubMed](#)]
58. Yuan, Y.; Call, M.K.; Yuan, Y.; Zhang, Y.; Fischesser, K.; Liu, C.Y.; Kao, W.W. Dexamethasone induces cross-linked actin networks in trabecular meshwork cells through noncanonical wnt signaling. *Investig. Ophthalmol. Vis. Sci.* **2013**, *54*, 6502–6509. [[CrossRef](#)] [[PubMed](#)]
59. Xue, W.; Comes, N.; Borrás, T. Presence of an established calcification marker in trabecular meshwork tissue of glaucoma donors. *Investig. Ophthalmol. Vis. Sci.* **2007**, *48*, 3184–3194. [[CrossRef](#)]
60. Xue, W.; Wallin, R.; Olmsted-Davis, E.A.; Borrás, T. Matrix GLA protein function in human trabecular meshwork cells: Inhibition of BMP2-induced calcification process. *Investig. Ophthalmol. Vis. Sci.* **2006**, *47*, 997–1007. [[CrossRef](#)]
61. Hu, H.; Tian, M.; Ding, C.; Yu, S. The C/EBP Homologous Protein (CHOP) Transcription Factor Functions in Endoplasmic Reticulum Stress-Induced Apoptosis and Microbial Infection. *Front. Immunol.* **2018**, *9*, 3083. [[CrossRef](#)]

62. Kim, I.; Xu, W.; Reed, J.C. Cell death and endoplasmic reticulum stress: Disease relevance and therapeutic opportunities. *Nat. Rev. Drug Discov.* **2008**, *7*, 1013–1030. [[CrossRef](#)]
63. Satyanarayana, A.; Kaldis, P. Mammalian cell-cycle regulation: Several Cdks, numerous cyclins and diverse compensatory mechanisms. *Oncogene* **2009**, *28*, 2925–2939. [[CrossRef](#)] [[PubMed](#)]
64. Ho, J.S.; Ma, W.; Mao, D.Y.; Benchimol, S. p53-Dependent transcriptional repression of c-myc is required for G1 cell cycle arrest. *Mol. Cell. Biol.* **2005**, *25*, 7423–7431. [[CrossRef](#)] [[PubMed](#)]
65. Yan, K.; Kalyanaraman, V.; Gautam, N. Differential ability to form the G protein betagamma complex among members of the beta and gamma subunit families. *J. Biol. Chem.* **1996**, *271*, 7141–7146. [[CrossRef](#)]
66. Ponten, F.; Jirstrom, K.; Uhlen, M. The Human Protein Atlas—a tool for pathology. *J. Pathol.* **2008**, *216*, 387–393. [[CrossRef](#)]
67. Kasukawa, T.; Masumoto, K.H.; Nikaido, I.; Nagano, M.; Uno, K.D.; Tsujino, K.; Hanashima, C.; Shigeyoshi, Y.; Ueda, H.R. Quantitative expression profile of distinct functional regions in the adult mouse brain. *PLoS ONE* **2011**, *6*, e23228. [[CrossRef](#)] [[PubMed](#)]
68. Valenzuela, D.M.; Murphy, A.J.; Friendewey, D.; Gale, N.W.; Economides, A.N.; Auerbach, W.; Poueymirou, W.T.; Adams, N.C.; Rojas, J.; Yasenachak, J.; et al. High-throughput engineering of the mouse genome coupled with high-resolution expression analysis. *Nat. Biotechnol.* **2003**, *21*, 652–659. [[CrossRef](#)]
69. Khrimian, L.; Obri, A.; Ramos-Brossier, M.; Rousseaud, A.; Moriceau, S.; Nicot, A.S.; Mera, P.; Kosmidis, S.; Karnavas, T.; Saudou, F.; et al. Gpr158 mediates osteocalcin's regulation of cognition. *J. Exp. Med.* **2017**, *214*, 2859–2873. [[CrossRef](#)]
70. Sutton, L.P.; Orlandi, C.; Song, C.; Oh, W.C.; Muntean, B.S.; Xie, K.; Filippini, A.; Xie, X.; Satterfield, R.; Yaeger, J.D.W.; et al. Orphan receptor GPR158 controls stress-induced depression. *eLife* **2018**, *7*, e33273. [[CrossRef](#)]
71. Tao, Y.X.; Conn, P.M. Chaperoning G protein-coupled receptors: From cell biology to therapeutics. *Endocr. Rev.* **2014**, *35*, 602–647. [[CrossRef](#)]
72. Lakin, N.D.; Jackson, S.P. Regulation of p53 in response to DNA damage. *Oncogene* **1999**, *18*, 7644–7655. [[CrossRef](#)]
73. Abuetaab, Y.; Wu, H.H.; Chai, C.; Al Yousef, H.; Persad, S.; Sergi, C.M.; Leng, R. DNA damage response revisited: The p53 family and its regulators provide endless cancer therapy opportunities. *Exp. Mol. Med.* **2022**, *54*, 1658–1669. [[CrossRef](#)]
74. Crawley, L.; Zamir, S.M.; Cordeiro, M.F.; Guo, L. Clinical options for the reduction of elevated intraocular pressure. *Ophthalmol. Eye Dis.* **2012**, *4*, 43–64. [[CrossRef](#)]
75. Erickson-Lamy, K.A.; Nathanson, J.A. Epinephrine increases facility of outflow and cyclic AMP content in the human eye in vitro. *Investig. Ophthalmol. Vis. Sci.* **1992**, *33*, 2672–2678.
76. Busch, M.J.; Kobayashi, K.; Hoyng, P.F.; Mittag, T.W. Adenylyl cyclase in human and bovine trabecular meshwork. *Investig. Ophthalmol. Vis. Sci.* **1993**, *34*, 3028–3034.
77. Crider, J.Y.; Sharif, N.A. Adenylyl cyclase activity mediated by beta-adrenoceptors in immortalized human trabecular meshwork and non-pigmented ciliary epithelial cells. *J. Ocul. Pharmacol. Ther.* **2002**, *18*, 221–230. [[CrossRef](#)] [[PubMed](#)]
78. McAuliffe-Curtin, D.; Buckley, C. Review of alpha adrenoceptor function in the eye. *Eye* **1989**, *3 Pt 4*, 472–476. [[CrossRef](#)]
79. Huang, Y.; Gil, D.W.; Vanscheeuwijk, P.; Stamer, W.D.; Regan, J.W. Localization of alpha 2-adrenergic receptor subtypes in the anterior segment of the human eye with selective antibodies. *Investig. Ophthalmol. Vis. Sci.* **1995**, *36*, 2729–2739.
80. Wax, M.B.; Molinoff, P.B.; Alvarado, J.; Polansky, J. Characterization of beta-adrenergic receptors in cultured human trabecular cells and in human trabecular meshwork. *Investig. Ophthalmol. Vis. Sci.* **1989**, *30*, 51–57.
81. Stamer, W.D.; Huang, Y.; Seftor, R.E.; Svensson, S.S.; Snyder, R.W.; Regan, J.W. Cultured human trabecular meshwork cells express functional alpha 2A adrenergic receptors. *Investig. Ophthalmol. Vis. Sci.* **1996**, *37*, 2426–2433.
82. Nakahara, M.; Shimozawa, M.; Nakamura, Y.; Irino, Y.; Morita, M.; Kudo, Y.; Fukami, K. A novel phospholipase C, PLC(eta)2, is a neuron-specific isozyme. *J. Biol. Chem.* **2005**, *280*, 29128–29134. [[CrossRef](#)] [[PubMed](#)]
83. Zhou, Y.; Wing, M.R.; Sondek, J.; Harden, T.K. Molecular cloning and characterization of PLC-eta2. *Biochem. J.* **2005**, *391*, 667–676. [[CrossRef](#)] [[PubMed](#)]
84. Stewart, A.J.; Morgan, K.; Farquharson, C.; Millar, R.P. Phospholipase C-eta enzymes as putative protein kinase C and Ca²⁺ signalling components in neuronal and neuroendocrine tissues. *Neuroendocrinology* **2007**, *86*, 243–248. [[CrossRef](#)]
85. Kanemaru, K.; Nakahara, M.; Nakamura, Y.; Hashiguchi, Y.; Kouchi, Z.; Yamaguchi, H.; Oshima, N.; Kiyonari, H.; Fukami, K. Phospholipase C-eta2 is highly expressed in the habenula and retina. *Gene Expr. Patterns* **2010**, *10*, 119–126. [[CrossRef](#)]
86. Laboute, T.; Zucca, S.; Holcomb, M.; Patil, D.N.; Garza, C.; Wheatley, B.A.; Roy, R.N.; Forli, S.; Martemyanov, K.A. Orphan receptor GPR158 serves as a metabotropic glycine receptor: mGlyR. *Science* **2023**, *379*, 1352–1358. [[CrossRef](#)]
87. Orlandi, C.; Posokhova, E.; Masuho, I.; Ray, T.A.; Hasan, N.; Gregg, R.G.; Martemyanov, K.A. GPR158/179 regulate G protein signaling by controlling localization and activity of the RGS7 complexes. *J. Cell Biol.* **2012**, *197*, 711–719. [[CrossRef](#)]
88. Filla, M.S.; Liu, X.; Nguyen, T.D.; Polansky, J.R.; Brandt, C.R.; Kaufman, P.L.; Peters, D.M. In vitro localization of TIGR/MYOC in trabecular meshwork extracellular matrix and binding to fibronectin. *Investig. Ophthalmol. Vis. Sci.* **2002**, *43*, 151–161.
89. Polansky, J.R.; Weinreb, R.N.; Baxter, J.D.; Alvarado, J. Human trabecular cells. I. Establishment in tissue culture and growth characteristics. *Investig. Ophthalmol. Vis. Sci.* **1979**, *18*, 1043–1049.
90. Polansky, J.R.; Wood, I.S.; Maglio, M.T.; Alvarado, J.A. Trabecular meshwork cell culture in glaucoma research: Evaluation of biological activity and structural properties of human trabecular cells in vitro. *Ophthalmology* **1984**, *91*, 580–595. [[CrossRef](#)]
91. Nguyen, T.D.; Chen, P.; Huang, W.D.; Chen, H.; Johnson, D.; Polansky, J.R. Gene structure and properties of TIGR, an olfactomedin-related glycoprotein cloned from glucocorticoid-induced trabecular meshwork cells. *J. Biol. Chem.* **1998**, *273*, 6341–6350. [[CrossRef](#)]

92. Stamer, W.D.; Seftor, R.E.; Williams, S.K.; Samaha, H.A.; Snyder, R.W. Isolation and culture of human trabecular meshwork cells by extracellular matrix digestion. *Curr. Eye Res.* **1995**, *14*, 611–617. [[CrossRef](#)]
93. Stamer, D.W.; Roberts, B.C.; Epstein, D.L.; Allingham, R.R. Isolation of primary open-angle glaucomatous trabecular meshwork cells from whole eye tissue. *Curr. Eye Res.* **2000**, *20*, 347–350. [[CrossRef](#)] [[PubMed](#)]
94. Keller, K.E.; Bhattacharya, S.K.; Borrás, T.; Brunner, T.M.; Chansangpetch, S.; Clark, A.F.; Dismuke, W.M.; Du, Y.; Elliott, M.H.; Ethier, C.R.; et al. Consensus recommendations for trabecular meshwork cell isolation, characterization and culture. *Exp. Eye Res.* **2018**, *171*, 164–173. [[CrossRef](#)]
95. Schmittgen, T.D.; Livak, K.J. Analyzing real-time PCR data by the comparative C(T) method. *Nat. Protoc.* **2008**, *3*, 1101–1108. [[CrossRef](#)]
96. Buie, L.K.; Karim, M.Z.; Smith, M.H.; Borrás, T. Development of a model of elevated intraocular pressure in rats by gene transfer of bone morphogenetic protein 2. *Investig. Ophthalmol. Vis. Sci.* **2013**, *54*, 5441–5455. [[CrossRef](#)] [[PubMed](#)]
97. Duma, D.; Collins, J.B.; Chou, J.W.; Cidlowski, J.A. Sexually dimorphic actions of glucocorticoids provide a link to inflammatory diseases with gender differences in prevalence. *Sci. Signal* **2010**, *3*, ra74. [[CrossRef](#)]
98. Li, G.; Lee, C.; Agrahari, V.; Wang, K.; Navarro, I.; Sherwood, J.M.; Crews, K.; Farsiu, S.; Gonzalez, P.; Lin, C.W.; et al. In vivo measurement of trabecular meshwork stiffness in a corticosteroid-induced ocular hypertensive mouse model. *Proc. Natl. Acad. Sci. USA* **2019**, *116*, 1714–1722. [[CrossRef](#)] [[PubMed](#)]
99. Wang, W.H.; Millar, J.C.; Pang, I.H.; Wax, M.B.; Clark, A.F. Noninvasive measurement of rodent intraocular pressure with a rebound tonometer. *Investig. Ophthalmol. Vis. Sci.* **2005**, *46*, 4617–4621. [[CrossRef](#)]

Disclaimer/Publisher’s Note: The statements, opinions and data contained in all publications are solely those of the individual author(s) and contributor(s) and not of MDPI and/or the editor(s). MDPI and/or the editor(s) disclaim responsibility for any injury to people or property resulting from any ideas, methods, instructions or products referred to in the content.